蘆田知史[2,3]、田倉智之[4]、高後　裕[1]（旭川医科大学内科学講座　消化器・血液腫瘍制御内科学分野[1]、旭川医科大学消化管再生修復医学講座[2]、札幌東徳州会病院 IBD センター[3]、大阪大学大学院医学系研究科医療経済産業政策学[4]）

p-B)　臨床プロジェクト

B-(1)　診療標準化コアプロジェクト

B-(1)-1　潰瘍性大腸炎・クローン病の診断基準および重症度基準の改変　(10:30～10:45)

総括　松井敏幸　福岡大学筑紫病院消化器内科

軽症例の重症度推移－臨床調査個人票電子化データ解析より

○桑原絵里加[1]、中村孝裕[1]、西脇祐司[1]、井上　詠[2]、長堀正和[3]、渡辺　守[3]、松井敏幸[4]（東邦大学医学部社会医学講座衛生学分野[1]、慶應義塾大学病院予防医療センター[2]、東京医科歯科大学消化器病態学[3]、福岡大学筑紫病院消化器内科[4]）

B-(1)-2　診療ガイドライン作成・改訂 (10:45～11:05)

総括　上野文昭　大船中央病院消化器肝臓病センター

日本消化器病学会との共同開発による炎症性腸疾患診療ガイドライン改訂：直面している問題点

○上野文昭[1]、渡邉聡明[2]、松井敏幸[3]、渡辺　守[4]、（大船中央病院[1]、東京大外科[2]、福岡大筑紫病院消化器内科[3]、東京医歯大消化器内科[4]）

炎症性腸疾患診療ガイドラインの改訂：現在の進捗状況

○上野文昭[1]、渡邉聡明[2]、井上　詠[3]、小俣富美雄[4]、加藤　順[5]、国崎玲子[6]、小金井一隆[7]、小林清典[8]、小林健二[9]、猿田雅之[10]、仲瀬裕志[11]、長堀正和[12]、平井郁仁[13]、本谷　聡[14]、松井敏幸[13]（大船中央病院[1]、東京大外科[2]、慶應義塾大予防医療センター[3]、聖路加国際病院[4]、和歌山県立医大第２内科[5]、横浜市大市民総合医療センターIBD センター[6]、横浜市立市民病院外科[7]、北里大東病院消化器内科[8]、聖路加国際病院一般内科[9]、慈恵医大消化器内科[10]、京都大消化器内科[11]、東京医歯大消化器内科[12]、福岡大筑紫病院消化器内科[13]、札幌厚生病院 IBD センター[14]）

B-(1)-3　標準化を目指した治療指針の改訂 (11:05～11:35)

総括　中村志郎　兵庫医科大学内科下部消化管科

治療の標準化を目指した潰瘍性大腸炎治療指針の改訂

○中村志郎[1]、杉田　昭[2]、余田　篤[3]、蘆田知史[4]、安藤　朗[5]、伊藤裕章[6]、押谷伸英[7]、金井隆典[8]、鈴木康夫[9]、長堀正和[10]、松井敏幸[11]、佐々木巌[12]、友政　剛[13]、田尻　仁[14]、福永　健[1]、樋田信幸[1]（兵庫医科大学内科学下部消化管科[1]、横浜市民病院外科[2]、大阪医科大学小児科[3]、札幌東徳洲会病院 IBD センター[4]、滋賀医科大学消化器内科[5]、錦秀会インフュージョンクリニック[6]、泉大津市立病院消化器内科[7]、慶応義塾大学消化器内科[8]、東邦大学佐倉病院消化器病センター[9]、東京医科歯科大学消化器病態学[10]、福岡大学筑紫病院消化器内科[11]、みやぎ健診プラザ[12]、パルこどもクリニック[13]、大阪府立急性期・総合医療センター小児科[14]）

治療の標準化を目指したクローン病治療指針の改訂

○中村志郎[1]、杉田　昭[2]、余田　篤[3]、蘆田知史[4]、安藤　朗[5]、伊藤裕章[6]、押谷伸英[7]、金井隆典[8]、鈴木康夫[9]、長堀正和[10]、松井敏幸[11]、佐々木巌[12]、友政　剛[13]、田尻　仁[14]、福永　健[1]、樋田信幸[1]（兵庫医科大学内科学下部消化管科[1]、横浜市民病院外科[2]、大阪医科大学小児科[3]、札幌東徳洲会病院 IBD センター[4]、滋賀医科大学消化器内科[5]、錦秀会インフュージョンクリニック[6]、泉大津市立病院消化器内科[7]、慶応義塾大学消化器内科[8]、東邦大学佐倉病院消化器病センター[9]、東京医科歯科大学消化器病態学[10]、福岡大学筑紫病院消化器内科[11]、みやぎ健診プラザ[12]、パルこどもクリニック[13]、大阪府立急性期・総合医療センター小児科[14]）

潰瘍性大腸炎、クローン病外科治療指針の改訂

○杉田　昭[1]、亀岡信悟[2]、二見喜太郎[3]、根津理一郎[4]、藤井久男[5]、楠　正人[6]、舟山裕士[7]、渡邉聡明[8]、福島浩平[9]、板橋道朗[10]、池内浩基[11]、佐々木巌[12]、中村志郎[13]（横浜市立市民病院炎症性腸疾患センター[1]、東京女子医大第２外科[2]、福岡大学筑紫病院外科[3]、西宮市立中央病院外科[4]、奈良県立医科大学中央内視鏡

超音波部[5]、三重大学消化管小児外科学[6]、東北労災病院大腸肛門外科[7]、東京大学大腸肛門外科[8]、東北大学分子病態外科[9]、東京女子医大第２外科[10]、兵庫医科大学下部消化管外科[11]、みやぎ健診プラザ[12]、兵庫医科大学内科学下部消化管科[13])

B-(2)　画期的な診断・治療の開発プロジェクト　－診断面からー

B-(2)-1　新たなデバイスを用いたクローン病小腸病変の診断と治療（11:35～12:10）

総括　松本主之　岩手医科大学内科学講座消化器内科消化管分野

クローン病の小腸狭窄に対する内視鏡的拡張療法－多施設共同前向き試験の登録終了の報告と現状－

○平井郁仁[1]、松本主之[2]、松井敏幸[1]（福岡大学筑紫病院消化器内科[1]、岩手医科大学内科学講座消化器内科消化管分野[2])

クローン病小腸病変に対するバルーン小腸内視鏡とMREの比較試験、Progress Study：国内多施設共同試験

○渡辺憲治[1]、十河光栄[1]、山上博一[1]、竹内　健[2]、鈴木康夫[2]、矢野智則[3]、歌野健一[4]、山本博徳[3]、平井郁仁[5]、松井敏幸[5]、長沼　誠[6]、日比紀文[7]、大塚和朗[8]、渡辺　守[8]（大阪市立大学大学院医学研究科消化器内科学[1]、東邦大学医療センター佐倉病院内科[2]、自治医科大学消化器内科[3]、福島県立医科大学会津医療センター小腸大腸肛門科[4]、福岡大学筑紫病院消化器内科[5]、慶應義塾大学医学部消化器内科[6]、北里大学北里研究所病院炎症性腸疾患先進治療センター[7]、東京医科歯科大学消化器病態学[8])

本邦クローン病におけるカプセル内視鏡所見の検討-多施設共同研究に関する中間報告-

○松本主之[1]、江崎幹宏[2]、渡辺　守[3]（岩手医科大学内科学講座消化器内科消化管分野[1]、九州大学病態機能内科学[2]、東京医科歯科大学消化器病態学[3])

＜昼食・幹事会＞　（12:10～13:00）

B-(2)-2　癌サーベイランス法の確立（13:00～13:25）

総括　渡邉聡明　東京大学臓器病態外科学講座腫瘍外科学

潰瘍性大腸炎に対する癌サーベイランス法の確立

○渡邉聡明[1]、味岡洋一[2]、武林　亨[3]、井上永介[4]、飯塚文瑛[5]、五十嵐正広[6]、岩男　泰[7]、大塚和朗[17]、工藤進英[8]、小林清典[9]、佐田美和[9]、田中信治[10]、友次直輝[11]、樋田信幸[12]、平田一郎[13]、松本主之[14]、渡辺憲治[15]、上野文昭[16]、渡辺　守[17]、日比紀文[18]（東京大学大学院医学系研究科・医学部臓器病態外科学講座腫瘍外科学[1]、新潟大学大学院医歯学総合研究科分子・診断病理学分野[2]、慶応義塾大学医学部衛生学公衆衛生学[3]、北里大学薬学部臨床統計[4]、東京女子医科大学消化器病センター[5]、癌研有明病院内科[6]、慶應義塾大学内科[7]、昭和大学横浜市北部病院消化器センター[8]、北里大学東病院内科[9]、広島大学病院内視鏡診療科[10]、慶應義塾大学クリニカルリサーチセンター[11]、兵庫医科大学下部消化管科[12]、藤田保健衛生大学消化管内科[13]、岩手医科大学内科学講座消化器内科消化管分野[14]、大阪市立大学医学部消化器内科[15]、大船中央病院・消化器肝臓病センター[16]、東京医科歯科大学消化器病態学[17]、北里大学北里研究所病院炎症性腸疾患先進治療センター[18])

クローン病に合併した大腸癌のsurveillance program確立の検討（痔瘻癌を含む）

－多施設共同研究によるpilot studyの中間報告（第4報）－

○杉田　昭[1]、小金井一隆[1]、二見喜太郎[2]、舟山裕士[3]、池内浩基[4]、根津理一郎[5]、板橋道朗[6]、水島恒和[7]、荒木俊光[8]、渡邉聡明[9]、福島浩平[10]、佐々木巌[11]（横浜市立市民病院炎症性腸疾患センター[1]、福岡大学筑紫病院外科[2]、東北労災病院大腸肛門外科[3]、兵庫医科大学下部消化管外科[4]、西宮市立中央病院外科[5]、東京女子医大第２外科[6]、大阪大学消化器外科[7]、三重大学消化管小児外科学[8]、東京大学大腸肛門外科[9]、東北大学分子病態外科[10]、みやぎ健診プラザ[11])

B-(3)　画期的な診断・治療の開発プロジェクト　－治療面から－

B-(3)-1　難治性炎症性腸疾患に対する新規治療の位置づけ　(13:25～13:50)

総括　日比紀文　北里大学北里研究所病院炎症性腸疾患先進治療センター

多施設共同医師主導型臨床試験「難治性潰瘍性大腸炎に対するタクロリムスとインフリキシマブの治療効果比較試験」

○松岡克善[1]、長沼　誠[1]、金井隆典[1]、日比紀文[2]、渡辺　守[3]、樋田信幸[4]、松浦　稔[5]、猿田雅之[6]、朝倉敬子[7]
（慶應義塾大学消化器内科[1]、北里大学北里研究所病院炎症性腸疾患先進治療センター[2]、東京医科歯科大学消化器病態学[3]、兵庫医科大学内科下部消化管科[4]、京都大学医学部消化器内科[5]、東京慈恵会医科大学消化器・肝臓内科[6]、東京大学大学院医学系研究科公共健康医学専攻疫学保健学講座[7]）

多施設共同医師主導型臨床試験「インフリキシマブ治療によって寛解維持された潰瘍性大腸炎患者に対するインフリキシマブ治療の中止および継続群の寛解維持率比較研究-HAYABUSA-」：進捗状況

○小林　拓[1]、久松理一[2]、仲瀬裕志[3]、平井郁仁[4]、松本主之[5]、本谷　聡[6]、渡辺憲治[7]、日比紀文[1]（北里大学北里研究所病院炎症性腸疾患先進治療センター[1]、慶應義塾大学医学部消化器内科[2]、京都大学消化器内科[3]、福岡大学筑紫病院消化器内科[4]、岩手医科大学内科学講座消化器内科消化管分野[5]、JA北海道厚生連札幌厚生病院IBDセンター[6]、大阪市立大学消化器内科[7]）

B-(3)-2　クローン病に対する適切な免疫調節剤投与法、インフリキシマブ二次無効例に対する対処 (13:50～14:35)

総括　鈴木康夫　東邦大学医療センター佐倉病院内科

クローン病に対するアダリムマブと免疫調節剤併用療法の検討：進捗状況

○松本主之[1]、仲瀬裕志[2]、渡辺憲治[3]、久松理一[4]、日比紀文[5]、渡辺　守[6]
(岩手医科大学内科学講座消化器内科消化管分野[1]、京都大学消化器内科[2]、大阪市立大学消化器内科[3]、慶應義塾大学消化器内科[4]、北里研究所病院炎症性腸疾患先進治療センター[5]、東京医科歯科大学消化器病態学[6])

インフリキシマブによる寛解維持治療における効果不十分なクローン病患者を対象とした栄養療法併用効果確認試験（CERISIER　Trial）（多施設共同研究）

○久松理一[1]、中村志郎[2]、長堀正和[3]、横山　薫[4]、国崎玲子[5]、辻川知之[6]、仲瀬裕志[7]、渡辺憲治[8]、本谷　聡[9]、蘆田知史[10]、山本博徳[11]、平石秀行[12]、屋嘉比康治[13]、勝野達郎[14]、鈴木康夫[15]、大草敏史[16]、飯塚文瑛[17]、中井勝彦[18]、横山　正[19]、平田一郎[20]、山本隆行[21]、飯島英樹[22]、樋口和秀[23]、小坂　正[24]、春間　賢[25]、平岡佐規子[26]、田中信治[27]、河内修治[28]、安藤　朗[6]、渡辺　守[3]、日比紀文[29]（慶應義塾大学消化器内科[1]、兵庫医科大学消化器内科[2]、東京医科歯科大学消化器病態学[3]、北里大学東病院消化器内科[4]、横浜市立大学炎症性腸疾患（IBD）センター[5]、滋賀医科大学消化器内科[6]、京都大学内科系　消化器内科学講座[7]、大阪市立大学消化器内科[8]、札幌厚生病院IBDセンター[9]、札幌東徳洲会病院IBDセンター[10]、自治医科大学消化器内科[11]、獨協医科大学消化器内科[12]、埼玉医科大学医療センター消化器・肝臓内科[13]、千葉大学消化器内科[14]、東邦大学佐倉病院消化器内科[15]、東京慈恵会医科大学柏病院消化器・肝臓内科[16]、東京女子医科大学消化器内科[17]、松田病院胃腸・肛門外科[18]、横山胃腸科病院[19]、藤田保健衛生大学消化器内科[20]、四日市社会保険病院IBDセンター[21]、大阪大学消化器内科[22]、大阪医科大学消化器内科[23]、大和病院[24]、川崎医科大学食道・胃腸内科[25]、岡山大学消化器・肝臓内科[26]、広島大学内視鏡診療科[27]、松山赤十字病院消化器内科[28]、北里大学北里研究所病院炎症性腸疾患先進治療センター[29]

多施設共同医師主導型臨床研究「アダリムマブと免疫調節剤併用中の寛解クローン病患者における免疫調節剤休薬の検討-Diamond2」

○久松理一[1]、松本主之[2]、仲瀬裕志[3]、渡辺憲治[4]、渡辺　守[5]、日比紀文[6]（慶應義塾大学医学部消化器内科[1]、岩手医科大学内科学講座消化器内科消化管分野[2]、京都大学消化器内科・内視鏡部[3]、大阪市立大学消化器内科[4]、東京医科歯科大学消化器病態学[5]、北里大学北里研究所病院炎症性腸疾患先進治療センター[6]）

特殊型炎症性腸疾患におけるアダリムマブとステロイドの前向き無作為化比較試験、
Castle Study： 国内多施設共同試験

○渡辺憲治[1]、松本主之[2]、仲瀬裕志[3]、久松理一[4]、平井郁仁[5]、小林清典[6]、日比紀文[7]、渡辺　守[8]（大阪市立大大学院医学研究科消化器内科学[1]、岩手医科大学内科学講座消化器内科消化管分野[2]、京都大学消化器内科・内視鏡部[3]、慶應義塾大学医学部消化器内科[4]、福岡大学筑紫病院消化器内科[5]、北里大学東病院消化器内科[6]、北里大学北里研究所病院炎症性腸疾患先進治療センター[7]、東京医科歯科大学消化器病態学[8]）

B-(3)-3　外科治療の現状と工夫（14:35～15:30）

総括　杉田　昭　横浜市立市民病院外科

外科治療の現状、工夫、予後 -プロジェクト研究の現状と方針-

○杉田　昭[1]、亀岡信悟[2]、二見喜太郎[3]、根津理一郎[4]、藤井久男[5]、楠　正人[6]、舟山裕士[7]、渡邉聡明[8]、福島浩平[9]、板橋道朗[2]、池内浩基[11]、佐々木巌[12]（横浜市立市民病院炎症性腸疾患センター[1]、東京女子医大第２外科[2]、福岡大学筑紫病院外科[3]、西宮市立中央病院外科[4]、奈良県立医科大学中央内視鏡超音波部[5]、三重大学消化管、小児外科学[6]、東北労災病院大腸肛門外科[7]、東京大学大腸肛門外科[8]、東北大学分子病態外科[9]、兵庫医科大学下部消化管外科[11]、みやぎ健診プラザ[12]）

クローン病術後療法に関する調査研究―インフリキシマブ併用療法・術後管理

○福島浩平[1]、羽根田祥[2]、渡辺和宏[2]、長尾宗徳[2]、神山篤史[2]、鈴木秀幸[2]、舟山裕士[3]、杉田　昭[4]、二見喜太郎[5]、畠山勝義[6]、藤井久男[7]、吉岡和彦[9]、亀岡信悟[10]、渡邉聡明[11]、楠　正人[12]、池内浩基[13]、中村志郎[14]、鈴木康夫[15]、木内喜孝[16]、渡辺　守[17]、佐々木巌[18]（東北大学大学院消化管再建医工学・分子病態外科学分野[1]、東北大学大学院生体調節外科学分野[2]、東北労災病院大腸肛門外科[3]、横浜市民病院外科[4]、福岡大学筑紫病院外科[5]、新潟大学消化器・一般外科[6]、奈良県立医科大学中央内視鏡・超音波部[7]、兵庫医科大学外科[8]、関西医科大学付属香里病院外科[9]、東京女子医科大学第二外科[10]、東京大学腫瘍外科[11]、三重大学消化管・小児外科学[12]、兵庫医科大学IBDセンター外科[13]、兵庫医科大学IBDセンター内科科[14]、東邦大学医療センター佐倉病院内科[15]、東北大学保健管理センター[16]、東京医科歯科大学消化器病態学[17]、みやぎ健診プラザ[18]）

回腸嚢炎に関する調査研究―「寛解」の定義(案)

○福島浩平[1]、羽根田祥[2]、渡辺和宏[2]、鈴木秀幸[2]、長尾宗紀[2]、神山篤史[2]、舟山裕士[3]、杉田　昭[4]、二見喜太郎[5]、藤井久男[7]、池内浩基[8]、小金井一隆[4]、飯合恒夫[6]、東大二郎[5]、吉岡和彦[9]、亀岡信悟[10]、板橋道朗[10]、渡邉聡明[11]、楠　正人[12]佐々木巌[13]（東北大学大学院消化管再建医工学・分子病態外科学分野[1]、東北大学大学院生体調節外科学分野[2]、東北労災病院大腸肛門外科[3]、横浜市民病院外科[4]、福岡大学筑紫病院外科[5]、白根健生病院[6]、奈良県立医科大学中央内視鏡・超音波部[7]、兵庫医科大学IBDセンター外科[8]、関西医科大学付属香里病院外科[9]、東京女子医科大学第二外科[10]、東京大学腫瘍外科[11]、三重大学消化管・小児外科学[12]、みやぎ健診プラザ[13]）

高齢者潰瘍性大腸炎に対する手術の検討 - 手術適応、手術時期、手術術式、予後のアンケート調査（中間報告） -

○杉田　昭[1]、亀岡信悟[2]、二見喜太郎[3]、根津理一郎[4]、藤井久男[5]、楠　正人[6]、舟山裕士[7]、渡邉聡明[8]、福島浩平[9]、板橋道朗[10]、池内浩基[11]、佐々木巌[12]（横浜市立市民病院炎症性腸疾患センター[1]、東京女子医大第２外科[2]、福岡大学筑紫病院外科[3]、西宮市立中央病院外科[4]、奈良県立医科大学中央内視鏡超音波部[5]、三重大学消化管、小児外科学[6]、東北労災病院大腸肛門外科[7]、東京大学大腸肛門外科[8]、東北大学分子病態外科[9]、東京女子医大第２外科[10]、兵庫医科大学下部消化管外科[11]、みやぎ健診プラザ[12]）

クローン病肛門部病変の重症度分類について

○二見喜太郎、東大二郎、石橋由紀子（福岡大学筑紫病院外科）

B-(4)　診療に伴う合併症/副作用および特殊型への対策プロジェクト

B-(4)-1　潰瘍性大腸炎合併サイトメガロウイルス腸炎および血栓症（15:30～16:15）

総括　鈴木康夫　東邦大学医療センター佐倉病院内科

潰瘍性大腸炎に対するインフリキシマブ効果予測と長期経過

○鈴木康夫、岩佐亮太、山田哲弘、竹内　健（東邦大学医療センター佐倉病院内科）

CMV感染合併潰瘍性大腸炎診断における大腸組織内CMV-DNA定量評価の意義 － 免疫組織染色法との比較検討 －

鈴木 康夫[1]、平山圭穂[1]、山田哲弘[1]、○仲瀬裕志[2]、石黒 陽[3]、大宮美香[4]、長沼　誠[5]、松岡克善[5]、長堀正和[6]、福知　工[7]、平井郁仁[8]（東邦大学医療センター佐倉病院内科[1]、京都大学消化器内科[2]、弘前病院消化器血液内科[3]、関西医科大学内科[4]、慶應義塾大学消化器内科[5]、東京医科歯科大学消化器病態学[6]、済生会中津病院消化器内科[7]、福岡大学筑紫病院消化器内科[8]）

潰瘍性大腸炎術後の消化管出血について（サイトメガロウィルス腸炎を含む）

福島浩平[1]、鈴木康夫[2]、羽根田祥[3]、渡辺和宏[3]、○神山篤史[3]、長尾宗紀[3]、舟山裕士[4]、杉田　昭[5]、二見喜太郎[6]、藤井久男[7]、池内浩基[8]、吉岡和彦[9]、板橋道朗[10]、渡邉聡明[11]、楠　正人[12]、橋本拓造[10]、辰巳健志[5]、内野　基[8]、河口貴昭[13]、高津典孝[14]、石黒　陽[15]、仲瀬裕志[16]、大宮美香[17]、平井郁仁[14]、池田圭祐[18]、山田哲弘[2]、松岡克善[19]、長沼　誠[19]、福地　工[20]、長堀正和[21]、渡辺　守[21]（東北大学大学院消化管再建医工学・分子病態外科学分野[1]、東邦大学医療センター佐倉病院内科[2]、東北大学大学院生体調節外科学分野[3]、東北労災病院大腸肛門外科[4]、横浜市民病院外科[5]、福岡大学筑紫病院外科[6]、奈良県立医科大学中央内視鏡・超音波部[7]、兵庫医科大学外科[8]、関西医科大学付属枚方病院外科[9]、東京女子医科大学第二外科[10]、帝京大学消化器外科[11]、三重大学消化管・小児外科学[12]、社会保険中央病院内科[13]、福岡大学消化器内科筑紫病院消化器内科[14]、弘前大学光学医療診療部[15]、京都大学消化器内科[16]、関西医科大学香里病院消化器内科[17]、福岡大学筑紫病院病理[18]、慶應義塾大学医学部消化器内科[19]、大阪済生会中津病院消化器内科[20]、東京医科歯科大学消化器病態学[21]）

炎症性腸疾患における血栓症発症の頻度および危険因子に関する多施設共同研究の実施状況

○藤谷幹浩[1]、安藤勝祥[1]、伊藤貴博[1]、稲場勇平[1]、上野伸展[1]、盛一健太郎[1]、前本篤男[2,3]、蘆田知史[2,3]、田邊裕貴[4]、高後　裕[1]（旭川医科大学内科学講座　消化器・血液腫瘍制御内科学分野[1]、旭川医科大学消化管再生修復医学講座[2]、札幌東徳洲会病院IBDセンター[3]、国際医療福祉大学病院消化器内科[4]）

B-(4)-2　炎症性腸疾患にともなう感染症の現状とその対策（16:15～16:35）

総括　岡崎和一　関西医科大学　消化器・肝臓内科

我が国における炎症性腸疾患の急性増悪・再燃因子の前向き実態調査（特に感染症との関連性）

岡崎和一[1]、○大宮美香[1]、深田憲将[1]、佐々木誠人[2]、渡辺憲治[3]、大川清孝[4]、加賀谷尚史[5]、高添正和[6]、酒匂美奈子[6]、渡辺守[7]、長堀正和[7]、飯塚文瑛[8]、後藤秀実[9]、谷田諭史[9]、花井洋行[10]、飯田貴之[10]、平田一郎[11]、藤田浩史[11]、加藤　順[12]（関西医科大学内科学第三講座[1]、愛知医科大学消化器内科[2]、大阪市立大学消化器内科[3]、大阪市立十三市民病院[4]、金沢大学消化器内科[5]、社旗保険中央総合病院IBDセンター[6]、東京医科歯科大学消化器病態学[7]、東京女子医科大学IBDセンター[8]、名古屋市立大学消化器・代謝内科[9]、浜松南病院IBDセンター[10]、藤田保健衛生大学消化管内科[11]、和歌山県立医科大学第二内科[12]）

炎症性腸疾患におけるHBV感染の現状

坪内博仁[1,2]、○沼田政嗣[1]、森内昭博[1]、上村修司[1]、玉井　努[1]、船川慶太[1]、藤田　浩[1]、宇都浩文[1]、桶谷　眞[1]、井戸章雄[1]（鹿児島大学大学院 消化器疾患・生活習慣病学[1]、鹿児島市立病院[2]）

B-(4)-3　炎症性腸疾患と他臓器相関に関する臨床研究（16:35～16:55）

総括　岡崎和一　関西医科大学　消化器・肝臓内科

多施設共同観察研究　炎症性腸疾患に合併する自己免疫性膵炎の実態調査（最終報）

― 難治性膵疾患に関する調査研究班との共同研究 ―

○岡崎和一[1]、渡辺　守[2]、川　茂幸[3]、下瀬川　徹[4]（関西医科大学内科学第三講座[1]、東京医科歯科大学消化器病態学[2]、信州大学医学部内科学第二講座[3]、東北大学消化器内科[4]）

免疫修飾的治療下の炎症性腸疾患患者に対するインフルエンザワクチン接種の有効性の検討、中間報告

～「予防接種に関するワクチンの有効性・安全性等についての分析疫学研究：廣田班」との共同研究 ～

◯渡辺憲治[1]、松本紘子[1]、大藤さとこ[2]、萩原良恵[1]、山上博一[1]、荒川哲男[1]、廣田良夫[2]

(大阪市立大学大学院医学研究科消化器内科学[1]、公衆衛生学[2])

B-(4)-4　炎症性腸疾患患者の妊娠出産における現状とその対策 (16:55～17:10)

総括　三浦総一郎　防衛医科大学校内科学講座（穂苅量太）

妊娠出産の転帰と治療内容に関する多施設共同研究の状況

三浦総一郎[1]、◯穂苅量太[1]、高本俊介[1]、渡辺知佳子[1]、長堀正和[2]、渡辺　守[2]、松岡克善[3]、長沼　誠[3]、日比紀文[4]、本谷　聡[5]、樋田信幸[6]、国崎玲子[7]、高橋宏和[7]、吉村直樹[8]、飯塚文瑛[9]、藤盛健二[10]、猿田雅之[11]、谷田諭史[12]、藤山佳秀[13]、内藤裕二[14]、渡辺憲治[15]、飯島英樹[16]、上野義隆[17]、田中信治[17]、石原俊治[18]、杉田　昭[19]、池上幸治[20]、松本主之[20]、仲瀬裕志[21]、岡崎和一[22]、石黒　陽[23]、松本吏弘[24]、　嵜山敏男[25]、小林清典[26]、横山　薫[26]、松井敏幸[27]、鶴身小都絵[27]、加賀谷尚史[28]、井上拓也[29]（順不同）（防衛医科大学校内科[1]、東京医科歯科大学消化器病態学[2]、慶應義塾大学医学部消化器内科[3]、北里大学北里研究所病院炎症性腸疾患先進治療センター[4]、札幌厚生病院 IBD センター[5]、兵庫医科大学内科学下部消化管科[6]、横浜市立大学消化器内科[7]、社会保険中央総合病院内科[8]、東京女子医科大学 IBD センター（消化器内科）[9]、埼玉医大消化器肝臓内科[10]、慈恵会医科大学付属病院消化器・肝臓内科[11]、名古屋市立大学病院消化器内科[12]、滋賀医科大学消化器内科[13]、京都府立医科大学消化器内科[14]、大阪市立大学病院消化器内科[15]、大阪大学医学部付属病院消化器内科[16]、広島大学病院内視鏡診療科[17]、島根医科大学消化器内科[18]、横浜市民病院外科[19]、岩手医科大学内科学講座消化器内科消化管分野[20]、京都大学消化器内科[21]、関西医大消化器肝臓内科[22]、弘前大学光学医療科[23]、さいたま医療センター消化器科[24]、鹿児島大学医学部付属病院消化器内科[25]、北里大学東病院消化器内科[26]、福岡大学筑紫病院消化器内科[27]、金沢大学附属病院消化器内科[28]、大阪医科大学消化器内科[29])

B-(4)-5　高齢及び小児期発症炎症性腸疾患患者の治療指針の必要性　(17:10 ～17:30)

総括　三浦総一郎　防衛医科大学校内科学講座（穂苅量太）

高齢者炎症性腸疾患診療の現状把握 ― 前向き多施設共同研究の経過報告 ―

三浦総一郎[1]、◯高本俊介[1]、穂苅量太[1]、渡辺知佳子[1]、田中浩紀[2]、本谷　聡[2]、松本吏弘[3]、長堀正和[4]、渡辺　守[4]、松岡克善[5]、金井隆典[5]、小林　拓[6]、日比紀文[6]、横山　薫[7]、小林清典[7]、谷田諭史[8]、瀬戸山仁[9]、藤田　浩[9]、坪内博仁[9]、高橋晴彦[10]、松井敏幸[10]、加藤真吾[11]（順不同）（防衛医科大学校内科[1]、札幌厚生病院 IBD センター[2]、自治医科大学付属さいたま医療センター消化器科[3]、東京医科歯科大学消化器病態学[4]、慶應義塾大学医学部消化器内科[5]、北里大学北里研究所病院炎症性腸疾患先進治療センター[6]、北里大学東病院消化器内科[7]、名古屋市立大学病院消化器内科[8]、鹿児島大学医学部付属病院消化器内科[9]、福岡大学筑紫病院消化器内科[10]、埼玉医科大学総合医療センター消化器内科[11])

小児期発症炎症性腸疾患の治療に関する全国調査

◯清水俊明[1]、友政　剛[2]、田尻　仁[3]、国崎玲子[4]、石毛　崇[5]、山田寛之[6]、新井勝大[7]、大塚宜一[1]、余田　篤[8]、牛島高介[9]、青松友槻[8]、永田　智[10]、内田恵一[11]、竹内一夫[12]、穂刈量太[13]、三浦総一郎[13]、渡辺　守[14]

(順天堂大学医学部小児科[1]、パルこどもクリニック[2]、大阪府立急性期・総合医療センター小児医療センター[3]、横浜市立大学附属市民総合医療センター[4]、群馬大学大学院医学系研究科小児科学[5]、大阪府立母子センター消化器内分泌科[6]、国立成育医療研究センター消化器科[7]、大阪医科大学泌尿生殖発達医学講座小児科[8]、久留米大学医療センター小児科[9]、東京女子医科大学小児科[10]、三重大学医学部小児外科[11]、埼玉大学教育学部学校保健学講座[12]、防衛医科大学内科[13]、東京医科歯科大学消化器病態学[14])

事務局連絡

(17:30 終了予定)

懇親会 (17:30～)

Ⅰ．研究報告（続）

p-C）　基礎プロジェクト

C-(1)　診療に有用なバイオマーカー開発

C-(1)-1　免疫関連バイオマーカーの開発（9:00～9:30）

総括　竹田　潔　大阪大学大学院医学系研究科、千葉　勉　京都大学大学院医学研究科消化器内科学

虫垂リンパ組織の腸管恒常性維持における役割

○竹田　潔（大阪大学大学院医学系研究科免疫制御学）

クローン病における Th17 誘導性ミエロイド細胞の役割

○荻野崇之[1]、西村潤一[1]、香山尚子[2]、Soumik Barman[2]、植村　守[1]、畑　泰司[1]、竹政伊知朗[1]、水島恒和[1]、山本浩文[1]、土岐祐一郎[1]、森　正樹[1]、竹田　潔[2]（大阪大学大学院医学系研究科消化器外科[1]、大阪大学大学院医学系研究科免疫制御学[2]）

CXCR3 阻害剤の役割と治療応用

○石黒　陽[1,2]、櫻庭　裕丈[2]、蓮井　桂介[2]、平賀　寛人[2]、福田　眞作[2]
（国立病院機構弘前病院消化器血液内科[1]、弘前大学消化器血液内科[2]）

クローン病感受性遺伝子A20による腸炎惹起機構

○大島　茂、松沢　優、高原政宏、小林正典、仁部洋一、前屋舗千明、永石宇司、土屋輝一郎、岡本隆一、中村哲也、渡辺　守（東京医科歯科大学消化器病態学）

炎症性腸疾患の病態におけるリンパ管新生の関与炎症性腸疾患の病態におけるリンパ管新生の関与

○佐藤宏和[1]、成松和幸[1]、安武優一[1]、丸田紘一[1]、栗原千枝[1]、渡辺知佳子[1]、岡田義清[1]、碓井真吾[1]、冨田謙吾[1]、高本俊介[1]、永尾重昭[1]、穂苅量太[1]、三浦総一郎[2]（防衛医科大学校消化器内科[1]、防衛医科大学校[2]）

C-(1)-2　臨床的バイオマーカーの開発（9:30 ～9:54）

総括　日比紀文　北里大学北里研究所病院炎症性腸疾患先進治療センター

潰瘍性大腸炎に対する血球成分除去療法前後のケモカインプロファイリング

坪内博仁[1,2]、○上村修司[1]、小野陽平[1]、沼田政嗣[1]、瀬戸山仁[1]、藤田　浩[1]、井戸章雄[1]、嵜山敏男[3]、児玉眞由美[4]
（鹿児島大学大学院 消化器疾患・生活習慣病学[1]、鹿児島市立病院[2]、出水総合医療センター[3]、宮崎医療センター病院[4]）

腸炎における Serum - derived Hyaluronan - Associated Protein (SHAP) 発現

佐々木誠人、○山口純治、野田久嗣、春日井邦夫（愛知医科大学消化器内科（消化管部門））

腸管炎症バイオマーカーとしての Fecal lipocalin の意義

千葉　勉[1]、仲瀬裕志[1]、○松浦　稔[1]、吉野琢哉[1]（京都大学医学部　消化器内科[1]）

CAP 治療効果予測因子としての温感と皮膚還流圧の上昇

○飯塚政弘[1,2]、衛藤　武[2]、相良志穂[1]、沼田友華[3]、柳原　悠[3]、熊谷　誠[3]（秋田赤十字病院附属あきた健康管理センター[1]、秋田赤十字病院消化器科[2]、秋田赤十字病院臨床工学課[3]）

C-(1)-3　疾患特異的バイオマーカーの開発（9:54～10:06）

（総括　坪内博仁　鹿児島大学大学院医歯学総合研究科寄附講座　HGF 組織修復・再生医療学講座）

総括　渡辺　守　東京医科歯科大学消化器病態学

IBD バイオマーカーLRG の臨床応用に向けて

○新﨑信一郎[1]、飯島英樹[1]、松岡克善[2]、金井隆典[2]、辻井正彦[1]、竹原徹郎[1]、本田宏美[3]、三嶋　隆[3]、仲　哲治[3]
（大阪大学大学院医学系研究科・消化器内科学[1]、慶應義塾大学内科[2]、医薬基盤研究所・免疫シグナルプロジェクト[3]）

クローン病特異的バイオマーカーの検討-多施設共同研究

○光山慶一[1]、 松井敏幸[2]、 金城福則[3]、 牧山和也[4]、 坪内博仁[5] (久留米大学医学部消化器内科 IBD センター[1]、福岡大学筑紫病院消化器科[2]、琉球大学医学部光学医療診療部[3]、社会医療法人春回会井上病院[4]、鹿児島大学医学部消化器・生活習慣病学[5])

C-(1)-4 腸内細菌関連バイオマーカーの開発 (10:06～10:30)

総括 藤山佳秀 滋賀医科大学消化器内科

クローン病腸内細菌叢の pyrosequence (Illumina) 解析

○藤山佳秀[1]、安藤 朗[2]、辻川知之[3]、馬場重樹[1]、西田淳史[1]、高橋憲一郎[2]、藤本剛英[2] (滋賀医科大学消化器内科[1]、滋賀医科大学大学院消化器免疫[2]、滋賀医科大学総合内科学[3])

大腸全摘術後回腸嚢腸内細菌叢と抗菌剤服用の影響

○福島浩平[1]、小森佑奈[1]、佐々木健吾[1]、斎藤 喬[1]、神山篤史[2]、渡辺和宏[2]、羽根田祥[2]、長尾宗紀[2]、鈴木秀幸[2]、舟山裕士[3]、高橋賢一[3]、佐々木巌[4] (東北大学大学院消化管再建医工学・分子病態外科学分野[1]、東北大学大学院生体調節外科学分野[2]、東北労災病院大腸肛門外科[3]、みやぎ健診プラザ[4])

UC 患者腸液中の CMV-DNA 検出の検討

金城福則[1]、○伊良波 淳[1]、金城 徹[1]、岸本一人[2]、外間 昭[2]、上原綾子[2]、金城武士[2]、藤田次郎[2]
(琉球大学医学部附属病院光学医療診療部[1]、琉球大学医学部附属病院第一内科[2])

乳酸菌由来ポリリン酸を用いた新規炎症性腸疾患治療薬の臨床応用へ向けた開発研究

○藤谷幹浩[1]、上野伸展[1]、稲場勇平[1]、盛一健太郎[1]、前本篤男[2,3]、蘆田知史[2,3]、田邊裕貴[4]、高後 裕[1] (旭川医科大学内科学講座 消化器・血液腫瘍制御内科学分野[1]、旭川医科大学消化管再生修復医学講座[2]、札幌東徳洲会病院 IBD センター[3]、国際医療福祉大学病院消化器内科[4])

C-(1)-5 炎症による発癌バイオマーカーの開発 (10:30～11:00)

総括 味岡洋一 新潟大学院医歯学総合研究科分子診断病理学分野

潰瘍性大腸炎の炎症性発癌と DNA 損傷応答

○谷 優佑[1]、味岡洋一[1]、渡辺佳織里[1]、若井俊文[2]、山口尚之[1] (新潟大学大学院医歯学総合研究科分子診断病理学分野[1]、新潟大学大学院医歯学総合研究科消化器一般外科分野[2])

潰瘍性大腸炎の炎症粘膜における遺伝子メチル化の検討—臨床像との関連も含めて—

○田原智満、平田一郎、中野尚子、長坂光夫、中川義仁、大宮直木 (藤田保健衛生大学消化管内科)

オルガノイド培養系の確立と腸炎関連発がん機構の解明への活用

○南木康作[1]、佐藤俊朗[1]、中里圭宏[1]、武下達矢[1]、松岡克善[1]、矢島知治[1]、久松理一[1]、井上 詠[2]、岩男 泰[2]、長沼 誠[3]、緒方晴彦[3]、藤井正幸[4]、渡邉聡明[4]、金井隆典[1] (慶應義塾大学医学部内科学教室消化器内科[1]、慶應義塾大学医学部予防医療センター[2]、慶應義塾大学医学部内視鏡センター[3]、東京大学医学部腫瘍外科[4])

炎症性発癌におけるMFG-Eの役割

石原俊治、○楠 龍策、多田育賢、園山浩紀、岡 明彦、福廻陽彦、大嶋直樹、森山一郎、結城崇史、川島耕作、木下芳一
(島根大学医学部内科学講座第二)

粘液産生がんにおけるAtoh1発現の意義

○土屋 輝一郎、福島啓太、加納嘉人、堀田伸勝、日比谷秀爾、林 亮平、大島 茂、岡本隆一、永石宇司、中村哲也、渡辺 守 (東京医科歯科大学消化器病態学)

C-(2)　粘膜修復機構解析と治療応用　(11:00～11:18)

総括　有村　佳昭　札幌医科大学消化器・免疫・リウマチ内科学

MSC 依存性細胞増殖の機序

◯一色裕之、小野寺馨、永石歓和、今井浩三、篠村恭久、有村佳昭 (札幌医科大学消化器・免疫・リウマチ内科学)

Wnt5a peptide による大腸上皮の修復

◯内藤裕二[1]、高木智久[1]、◯内山和彦[1] (京都府立医科大学消化器内科)

腸管上皮幹細胞培養とその臨床応用技術開発

◯中村哲也、水谷知裕、福田将義、野崎賢吾、渡辺　守 (東京医科歯科大学消化器病態学)

Ⅱ．国立保健医療科学院挨拶

国立保健医療科学院健康危機管理研究部上席主任研究官　武村　真治　先生　(11:20～11:30)

事務局連絡

閉会挨拶

(11:40 終了予定)

Ⅶ.　研究成果の別刷

Mediterranean mimicker

Soichi Arasawa, Hiroshi Nakase, Yoshinao Ozaki, Norimitsu Uza, Minoru Matsuura, Tsutomu Chiba

Lancet 2012; 380: 2052

Department of Gastroenterology and Hepatology, Graduate School of Medicine, Kyoto University Kyoto, Japan (S Arasawa MD, H Nakase MD, Y Ozaki MD, N Uza MD, M Matsuura MD, T Chiba MD)

Correspondence to: Dr Hiroshi Nakase, Department of Gastroenterology and Hepatology, Graduate School of Medicine, Kyoto University, 54 Shogoin-Kawaharacho, Sakyo-ku, Kyoto-city, Kyoto, 606-8507, Japan
hiropy_n@kuhp.kyoto-u.ac.jp

See Online for appendix

In April, 2009, a 42-year-old woman presented to our department with recurrent febrile attacks (over 38°C) and diffuse abdominal pain that spontaneously subsided within 2–3 days. Laboratory tests showed leucocytosis and raised serum C-reactive protein. Colonoscopy showed discontinuous loss of fine vascular markings, erythema, and friable mucosa in the right hemicolon. Biopsy specimens showed no characteristic features of Crohn's disease or ulcerative colitis. A CT of the abdomen showed abnormal thickness of the colon wall. Capsule endoscopy showed no abnormality of the small intestine. Antisaccharomyces cerevisiae antibodies (ASCA) and antineutrophil cytoplasmic antibodies (ANCA) were negative. She was diagnosed with indeterminate colitis and initially given 4 g of mesalazine per day, followed by 1·5 g for maintenance. However, her symptoms continued and in July, 2009, she was given 40 mg of oral prednisolone daily to control her repeated episodes. Her symptoms subsided, and the dosage was tapered 4 weeks later. Mercaptopurine could not be used because of her intolerability to the drug.

However, symptoms recurred when the prednisolone dosage was lowered and she had to have ongoing adjustment of steroid doses. A colonscopy was then done 8 months later, which showed circumferentially erythematous mucosa with erosions in the caecum, longitudinal erosions with pseudopolyposis-like lesions in the right hemicolon, and no involvement of the rectum. The endoscopic features resembled Crohn's disease (figure A), but biopsy specimens showed no granuloma. Intestinal tuberculosis and other infectious diseases were excluded. She continued to have weekly febrile episodes, with severe abdominal pain and bilateral arthralgia of the wrists, elbows, and shoulders. We suspected familial Mediterranean fever because her symptoms met the Tel Hashomer major criteria of 2 recurrent typical attacks. After obtaining written informed consent, we did a genome sequencing examination for the Mediterranean fever gene (*MEFV*) mutation, which showed a heterozygous *MEFV* 910G>A point mutation. The mutation causes a Gly304Arg missense mutation on pyrin (see appendix). Familial Mediterranean fever was diagnosed and she was given colchicine. Her fever and pain promptly subsided, and prednisolone and mesalazine were stopped. In February, 2011, colonoscopy showed remarkable improvement of the mucosal inflammation in the colon (figure B). At last follow up in October, 2012 she was symptom free.

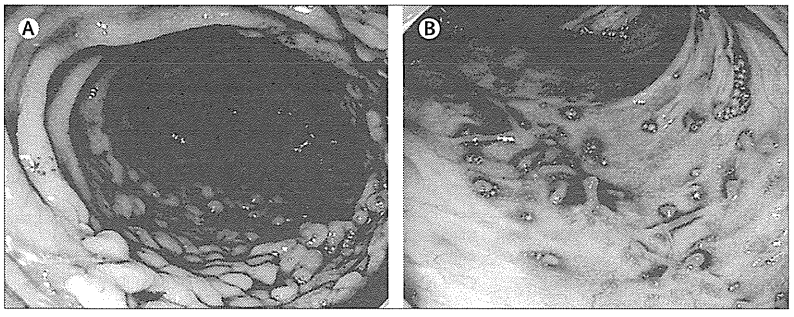

Figure: **Colonoscopy photography of of our patient**
(A) Transverse colon before treatment showing pseudopolypoid-like lesions of the transverse colon, and (B) after colchicine treatment with scar formation at the transverse colon.

Familial Mediterranean fever is a periodic inflammatory disease characterised by episodic febrile attacks and serositis. It is a monogenic Mendelian disease caused by an *MEFV* mutation on chromosome 16p13.3, which encodes pyrin.[1] Pyrin is a 781-aminoacid protein[2] which regulates the inflammatory response by blocking intracellular signal pathways via NF-κB or caspase 1. The absence of pyrin function due to mutated *MEFV* leads to the oversecretion of inflammatory cytokines.[3] The disease is rare in non-Mediterranean populations, which might mislead physicians to misdiagnose it as inflammatory bowel disease. Recent studies suggest an association between *MEFV* and inflammatory bowel disease,[4] although *MEFV* mutations make no important contribution to inflammatory bowel disease susceptibility.[5] Our patient showed colonic lesions mimicking Crohn's disease. The clinical course and genetic analysis led to a diagnosis of colonic lesions related to familial Mediterranean fever. Genetic analysis and colchicine treatment should be considered for patients with indeterminate colitis who do not respond to conventional inflammatory bowel treatment.

Contributors
SA, HN, YO, and NU looked after the patient. SA, HN, MM, and TC wrote the report. Written consent to publish was obtained.

References

1 Berdeli A, Mir S, Nalbantoglu S, et al. Comprehensive analysis of a large-scale screen for MEFV gene mutations: do they truly provide a "heterozygote advantage" in Turkey? *Genet Test Mol Biomarkers* 2011; **15**: 475–82.
2 Centola M, Wood G, Frucht D, et al. The gene for familial Mediterranean fever, MEFV, is expressed in early leukocyte development and is regulated in response to inflammatory mediators. *Blood* 2000; **95**: 3223–31.
3 Ting JP, Kastner DL, Hoffman HM. CATERPILLERs, pyrin and hereditary immunological disorders. *Nat Rev Immunol* 2006; **6**: 183–95.
4 Yıldırım B, Tuncer C, Kan D, et al. MEFV gene mutations and its impact on the clinical course in ulcerative colitis patients. *Rheumatol Int* 2011; **31**: 859–64.
5 Villani A, Lemire M, Louis E, et al. Genetic variation in the familial Mediterranean fever gene (MEFV) and risk for Crohn's disease and ulcerative colitis. *PLoS One* 2009; **4**: e7154.

ulate the methylaspartate cycle (see supporting online text).

Life in salt lakes is characterized by rare, ephemeral blooms of microorganisms (*1*), and under these circumstances, haloarchaea may accumulate substantial amounts of polyhydroxyalkanoate (*22*). Therefore, during starvation, having an anaplerotic acetyl-CoA assimilation pathway could be important for survival. In fact, most of the haloarchaeal genomes have genes for either the glyoxylate cycle (mostly clade II haloarchaea), the methylaspartate cycle (mostly clade I haloarchaea), or even both (for details, see figs. S5 and S6), which indicates their genetic potential to assimilate acetyl-CoA. As a proof of principle, we demonstrated characteristic reactions of the methylaspartate cycle in *Natrialba magadii* (clade I), but in contrast, key enzymes of the glyoxylate cycle were not detected (table S4).

Haloarchaea probably evolved from methanogens, whereupon they had to switch from a strictly anaerobic chemolithoautotrophic to an aerobic (photo)organoheterotrophic life-style (*23*, *24*). This switch was accompanied by a massive gene gain from the Bacteria domain (*23*). Haloarchaea that use the glyoxylate cycle have presumably acquired its key enzyme, ICL, by lateral gene transfer (*5*). Likewise, all key enzymes of the proposed methylaspartate cycle were derived via lateral gene transfer from bacterial genomes, where they originally participated in completely different metabolic processes (see supporting online text and figs. S7 to S10). This suggests that evolutionary tinkering (*25*) of acetate assimilation has occurred in haloarchaea, by which the methylaspartate cycle was assembled through the recombination of preexisting gene modules. Moreover, gene duplication and paralogy have presumably played an important role in evolutionary tinkering, as exemplified by RmAC0690 and RmAC1965 and as shown for other Archaea (*26*, *27*).

References and Notes

1. A. Oren, *Halophilic Microorganisms and Their Environments* (Kluwer Academic, Dordrecht, Netherlands, 2002).
2. H. L. Kornberg, H. A. Krebs, *Nature* **179**, 988 (1957).
3. A. Oren, P. Gurevich, *FEMS Microbiol. Lett.* **130**, 91 (1995).
4. J. A. Serrano, M. Camacho, M. J. Bonete, *FEBS Lett.* **434**, 13 (1998).
5. J. A. Serrano, M. J. Bonete, *Biochim. Biophys. Acta* **1520**, 154 (2001).
6. C. Bräsen, P. Schönheit, *Arch. Microbiol.* **175**, 360 (2001).
7. M. Falb *et al.*, *Extremophiles* **12**, 177 (2008).
8. M. J. Danson, H. J. Lamble, D. W. Hough, in *Archaea: Molecular and Cellular Biology*, R. Cavicchioli, Ed. (ASM Press, Washington, DC, 2007), pp. 260–287.
9. N. S. Baliga *et al.*, *Genome Res.* **14**, 2221 (2004).
10. T. J. Erb *et al.*, *Proc. Natl. Acad. Sci. U.S.A.* **104**, 10631 (2007).
11. T. J. Erb, G. Fuchs, B. E. Alber, *Mol. Microbiol.* **73**, 992 (2009).
12. Materials and methods are available as supporting material on *Science* Online.
13. J. Zarzycki, V. Brecht, M. Müller, G. Fuchs, *Proc. Natl. Acad. Sci. U.S.A.* **106**, 21317 (2009).
14. W. Buckel, G. Bröker, H. Bothe, A. J. Pierik, B. T. Golding, in *Chemistry and Biochemistry of B_{12}*, R. Banerjee, Ed. (Wiley, New York, 1999), pp. 757–781.
15. H. Connaris, J. B. Chaudhuri, M. J. Danson, D. W. Hough, *Biotechnol. Bioeng.* **64**, 38 (1999).
16. U. Johnsen *et al.*, *J. Biol. Chem.* **284**, 27290 (2009).
17. T. J. Erb, L. Frerichs-Revermann, G. Fuchs, B. E. Alber, *J. Bacteriol.* **192**, 1249 (2010).
18. W. Buckel, S. L. Miller, *Eur. J. Biochem.* **164**, 565 (1987).
19. L. Malki *et al.*, *J. Bacteriol.* **191**, 5196 (2009).
20. F. F. Hezayen, B. H. A. Rehm, R. Eberhardt, A. Steinbüchel, *Appl. Microbiol. Biotechnol.* **54**, 319 (2000).
21. T. Candela, A. Fouet, *Mol. Microbiol.* **60**, 1091 (2006).
22. J. G. Lillo, F. Rodriguez-Valera, *Appl. Environ. Microbiol.* **56**, 2517 (1990).
23. S. P. Kennedy, W. V. Ng, S. L. Salzberg, L. Hood, S. DasSarma, *Genome Res.* **11**, 1641 (2001).
24. É. Bapteste, C. Brochier, Y. Boucher, *Archaea* **1**, 353 (2005).
25. F. Jacob, *Science* **196**, 1161 (1977).
26. J. E. Tuininga *et al.*, *J. Biol. Chem.* **274**, 21023 (1999).
27. M. Daugherty, V. Vonstein, R. Overbeek, A. Osterman, *J. Bacteriol.* **183**, 292 (2001).
28. S. Shimizu, S. Ueda, K. Sato, in *Microbial Growth on C_1 Compounds*, R. L. Crawford, R. S. Hanson, Eds. (American Society for Microbiology, Washington, DC, 1984), pp. 113–117.
29. S. Vuilleumier *et al.*, *PLoS ONE* **4**, e5584 (2009).
30. R. Peyraud *et al.*, *Proc. Natl. Acad. Sci. U.S.A.* **106**, 4846 (2009).

31. The authors thank G. Fuchs, Freiburg, for his constant support and the innumerable discussions and suggestions during this work and for his critical reading of the manuscript and N. Gad'on and C. Ebenau-Jehle, Freiburg, for growing cells and maintaining the laboratory. The work of M.K. was supported by the Deutscher Akademischer Austausch Dienst. This work was supported by the Deutsche Forschungsgemeinschaft and Evonik-Degussa GmbH.

Supporting Online Material

www.sciencemag.org/cgi/content/full/331/6015/334/DC1
Materials and Methods
SOM Text
Figs. S1 to S10
Tables S1 to S7
References

16 August 2010; accepted 30 November 2010
10.1126/science.1196544

Induction of Colonic Regulatory T Cells by Indigenous *Clostridium* Species

Koji Atarashi,[1*] Takeshi Tanoue,[1*] Tatsuichiro Shima,[2] Akemi Imaoka,[2] Tomomi Kuwahara,[3] Yoshika Momose,[4] Genhong Cheng,[5] Sho Yamasaki,[6] Takashi Saito,[6] Yusuke Ohba,[7] Tadatsugu Taniguchi,[1] Kiyoshi Takeda,[8] Shohei Hori,[9] Ivaylo I. Ivanov,[10] Yoshinori Umesaki,[2] Kikuji Itoh,[4] Kenya Honda[1,11]†

CD4$^+$ T regulatory cells (T_{regs}), which express the Foxp3 transcription factor, play a critical role in the maintenance of immune homeostasis. Here, we show that in mice, T_{regs} were most abundant in the colonic mucosa. The spore-forming component of indigenous intestinal microbiota, particularly clusters IV and XIVa of the genus *Clostridium*, promoted T_{reg} cell accumulation. Colonization of mice by a defined mix of *Clostridium* strains provided an environment rich in transforming growth factor–β and affected Foxp3$^+$ T_{reg} number and function in the colon. Oral inoculation of *Clostridium* during the early life of conventionally reared mice resulted in resistance to colitis and systemic immunoglobulin E responses in adult mice, suggesting a new therapeutic approach to autoimmunity and allergy.

The mammalian gastrointestinal tract harbors numerous species of commensal bacteria that constitute the "microbiota." The microbiota interacts with the host immune system, inducing the accumulation of several different lymphocyte populations at mucosal sites (*1*, *2*). Recent reports have suggested that the induction of each lymphocyte subset may be regulated by a distinct component of the microbiota. For instance, segmented filamentous bacteria (SFB) strongly induce intestinal T helper 17 (T_H17) cells, which play a role in host resistance against intestinal pathogens and promote systemic autoimmunity (*3*–*5*).

CD4$^+$ regulatory T cells (T_{regs}) expressing the transcription factor forkhead box P3 (Foxp3) are present at higher frequencies in the gut lamina propria (LP), particularly in the colon, than in other organs (*6*) (fig. S1). It has been

[1]Department of Immunology, Graduate School of Medicine, University of Tokyo, Tokyo 113-0033, Japan. [2]Yakult Central Institute for Microbiological Research, Tokyo 186-8650, Japan. [3]Department of Molecular Bacteriology, Institute of Health Biosciences, University of Tokushima Graduate School, Tokushima 770-8503, Japan. [4]Department of Veterinary Public Health, University of Tokyo, Tokyo 113-8657, Japan. [5]Department of Microbiology, Immunology, and Molecular Genetics, David Geffen School of Medicine, University of California, Los Angeles, CA 90095, USA. [6]Laboratory for Cell Signaling, RIKEN Research Center for Allergy and Immunology, Yokohama, Kanagawa 230-0045, Japan. [7]Laboratory of Pathophysiology and Signal Transduction, Hokkaido University, Graduate School of Medicine, Sapporo 060-8638, Japan. [8]Laboratory of Immune Regulation, Graduate School of Medicine, Osaka University, Osaka 565-0871, Japan. [9]Research Unit for Immune Homeostasis, RIKEN Research Center for Allergy and Immunology, Yokohama, Kanagawa 230-0045, Japan. [10]Department of Microbiology and Immunology, Columbia University Medical Center, New York, NY 10032, USA. [11]Precursory Research for Embryonic Science and Technology (PRESTO), Japan Science and Technology Agency, Saitama 332-0012, Japan.

*These authors contributed equally to this work.
†To whom correspondence should be addressed. E-mail: kenya@m.u-tokyo.ac.jp

postulated that the number and function of mucosal T_{regs} are affected by the presence of intestinal bacteria. Indeed, daily treatment of mice with probiotic strains of bifidobacteria and lactobacilli modifies the inflammatory status of mice, presumably by inducing T_{regs} (*7–9*). Furthermore, colonization of mice with human commensal *Bacteroides fragilis* facilitates T_{reg} differentiation and interleukin-10 (IL-10) production (*10*). Given the importance of the community structure of "indigenous" microbial flora in the maintenance of intestinal homeostasis, and that its alteration (dysbiosis) correlates with inflammatory diseases (*11*), it is important to further investigate whether, and how, indigenous microflora affect the number and function of mucosal T_{regs}.

We first examined the appearance of T_{regs} during mouse ontogeny. The frequency of $Foxp3^+$ T_{regs} in colonic and small intestinal (SI) LP increased after weaning, whereas in inguinal lymph nodes (iLNs) it remained stable from the second week after birth (Fig. 1A). This temporal accumulation of intestinal T_{regs} suggested an influence of the intestinal microbiota. Therefore, we next examined germ-free (GF) mice. The percentage and absolute number of $Foxp3^+CD4^+$ T cells in SI, iLNs, Peyer's patches, and mesenteric LNs were unchanged, or increased, in GF mice and antibiotic-treated specific pathogen-free (SPF) mice compared with untreated SPF mice (Fig. 1B and fig. S2). These findings are consistent with previous observations that GF mice have increased or unchanged numbers of T_{regs} in SI (*12*, *13*). In contrast, a significant decrease in the number of $Foxp3^+$ T_{regs} was observed in the colonic LP of GF mice or antibiotic-treated mice compared with SPF mice (Fig. 1B and fig. S2). This decrease may be attributed to the absence of specific signaling events induced by intestinal microbes rather than to a defect in the development of gut-associated lymphoid tissues (fig. S3). Indeed, when GF mice were colonized with fecal suspensions from SPF mice ("conventionalization"), a marked increase in the frequency of T_{regs} was observed in colonic LP (Fig. 1C). Therefore, we conclude that interactions between indigenous microflora and the host play a critical role in the accumulation of colonic LP, but not SI LP, $Foxp3^+$ T_{regs}.

To determine whether a specific component of the intestinal flora induces colonic T_{reg} accumulation, we treated SPF mice with antibiotics that preferentially target Gram-positive (vancomycin) or Gram-negative (polymyxin B) bacteria (fig. S4). Compared with the controls, only mice treated with vancomycin had significantly lower frequencies of T_{regs} in the colon (Fig. 1D), suggesting a dominant role for Gram-positive commensal bacteria in T_{reg} accumulation. We next orally inoculated GF mice with 3% chloroform-resistant fecal microorganisms (spore-forming fraction) because this fraction has been shown to regulate intestinal T cell responses (*4*). Mice inoculated with chloroform-treated feces showed an increased number of T_{regs} (Fig. 1E) compara-

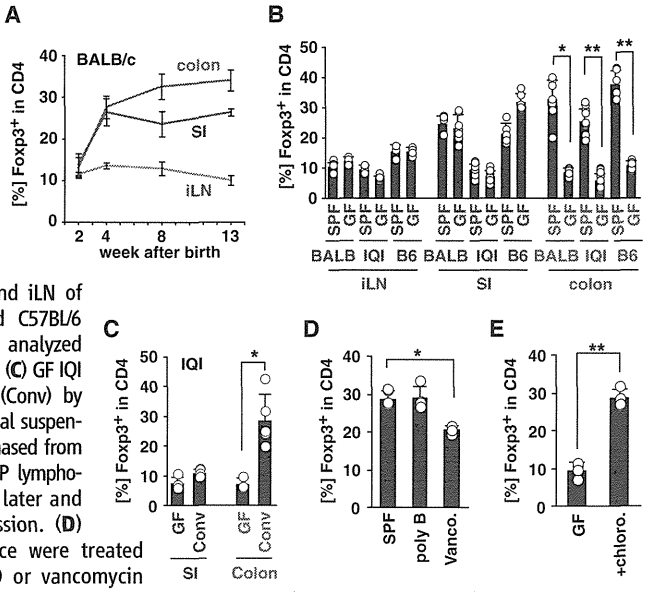

Fig. 1. Indigenous intestinal bacteria-dependent accumulation of colonic T_{regs}. (**A**) The percentage of $Foxp3^+$ cells within the $CD4^+$ cell population isolated from iLNs or LP of colon or SI of SPF BALB/c mice at the indicated age was analyzed by flow cytometry. (**B**) Lymphocytes from SI, colon, and iLN of 8-week-old BALB/c, IQI and C57BL/6 (B6) GF, and SPF mice were analyzed for CD4 and Foxp3 expression. (**C**) GF IQI mice were conventionalized (Conv) by oral administration of the fecal suspension from B6 SPF mice purchased from Jackson Laboratory. Colonic LP lymphocytes were isolated 3 weeks later and analyzed for Foxp3 expression. (**D**) Four-week-old SPF B6 mice were treated with polymyxin B (poly B) or vancomycin (Vanco) for 4 weeks and analyzed for the percentage of $Foxp3^+$ cells within the $CD4^+$ cell population. (**E**) GF mice were gavaged with chloroform-treated feces from SPF mice (+chloro) and analyzed for the percentage of $Foxp3^+$ cells within the $CD4^+$ cell population. Each circle in (B) to (E) represents an individual mouse, and error bars indicate the SD. Data were obtained from more than two independent experiments with similar results ($n \geq 4$ mice per group). $^*P < 0.01$; $^{**}P < 0.001$, unpaired *t* test.

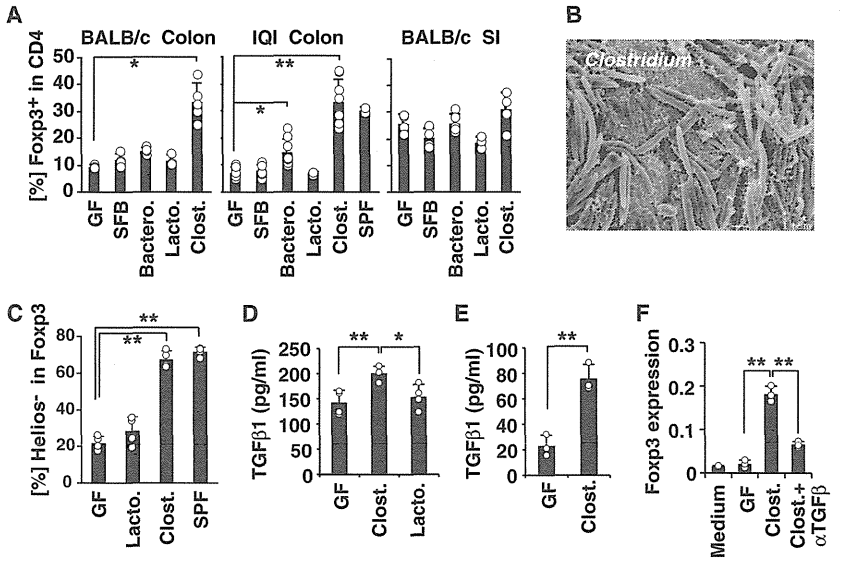

Fig. 2. Clostridia induce T_{reg} accumulation in colonic LP. (**A**) GF BALB/c or IQI mice were colonized with segmented filamentous bacteria (SFB), 16 strains of *Bacteroides* (Bactero.), 3 strains of *Lactobacillus* (Lacto.), or 46 strains of *Clostridium* (Clost.) for 3 weeks. The percentage of $Foxp3^+$ cells within the $CD4^+$ cell population in the colon and SI of individual mice was analyzed by flow cytometry ($n \geq 5$ mice per group). (**B**) Electron micrograph showing the proximal colon of Clost.-colonized B6 mice. (**C**) Lymphocytes from the colonic LP of indicated mice were analyzed for the expression of CD4, Foxp3, and Helios by flow cytometry. The percentage of $Helios^-$ cells within $Foxp3^+CD4^+$ lymphocytes is shown ($n = 4$ mice per group). (**D** and **E**) Whole colons (D) or IECs (E) from GF, Lacto.-, or Clost.-colonized mice were cultured for 24 hours. The concentration of TGF-β1 in the supernatant was determined by enzyme-linked immunosorbent assay (ELISA). (**F**) Splenic $CD4^+$ T cells were cultured with antibodies against CD3 and CD28 and 50% conditioned medium from cultured IECs isolated from GF or Clost.-colonized mice in the presence or absence of anti–TGF-β. After 5 days, T cells were collected and assayed for Foxp3 expression by real-time reverse transcription–polymerase chain reaction. Each circle represents a mouse or a sample, and error bars indicate the SD ($n \geq 3$ per group). $^*P < 0.02$; $^{**}P < 0.001$, unpaired *t* test. Data are representative of at least two independent experiments with similar results.

ble to that in SPF mice or GF mice gavaged with untreated feces (Fig. 1, B and C). Collectively, our results suggest that a specific component of the indigenous microbiota, belonging most likely to the Gram-positive, spore-forming fraction, plays a critical role in the induction of colonic T_{regs}.

Clostridia are one of the most prominent Gram-positive and spore-forming bacteria indigenous to the murine gastrointestinal tract (*14*). Moreover, *Clostridium* clusters IV and XIVa (also known as *Clostridium leptum* and *coccoides* groups, respectively) have been implicated in the maintenance of mucosal homeostasis and prevention of inflammatory bowel disease (IBD) (*15*, *16*). We therefore explored the link between clostridia and the accumulation of colonic T_{regs}. Clostridia became prominent after weaning and persisted in the adult animals, in contrast to *Lactobacillus* or *Enterobacteriaceae*, which were more abundant during the neonatal period and declined thereafter (fig. S5). Furthermore, *Clostridium* clusters IV and XIVa were most abundant in the cecum and proximal colon, which correlated well with the distribution of T_{regs} (fig. S6).

To directly examine the effect of *Clostridium* on the induction of colonic T_{regs}, we generated "gnotobiotic" mice by colonizing GF mice with fecal material obtained from mice colonized with a cocktail of 46 strains of *Clostridium* (*17*). *Clostridium*-colonized gnotobiotic mice exhibited a robust accumulation of T_{regs} in colonic LP; however, the frequency of SI T_{regs} was not affected (Fig. 2A and fig. S7, A and B). The 46 strains of *Clostridium* used were originally isolated from chloroform-treated fecal material from conventionally reared mice (*17*). These strains primarily belong to clusters IV and XIVa (*14*) (see also fig. S8). They are normally present in the intestine of several colonies of commercially available SPF mice and in that of mice housed in our own animal facility (fig. S9A). They mainly colonized the cecum and proximal colon (fig. S9B) and formed a thick layer on the mucosal epithelium (Fig. 2B). The induction of colonic T_{regs} was specific to *Clostridium*-colonized mice. Colonization with a cocktail of three strains of *Lactobacillus*, or with SFB, had little effect on the number of colonic T_{regs} (Fig. 2A and fig. S7, A and B). Furthermore, colonization by *B. fragilis*, which is reported to induce IL-10 production in T_{regs} (*10*), did not significantly affect the frequency of colonic T_{regs} (fig. S7C). A cocktail of 16 strains of *Bacteroides* spp. isolated from the murine intestine did induce a significant increase in the number of T_{regs} in the colon, although the magnitude was dependent on the background of the mice and was less than that seen in *Clostridium*-colonized mice (Fig. 2A and fig. S7, A and B).

A substantial fraction of $Foxp3^+$ T_{regs} observed in SPF or *Clostridium*-colonized mice was negative for Helios, a transcription factor reported to be expressed in thymus-derived natural T_{regs} (*18*), suggesting that many of these T_{regs} could be "induced T_{regs}" (iT_{regs}) (Fig. 2C and fig. S10A). A high number of T_{regs} was maintained for at least 4 months after colonization (fig. S10B). Furthermore, *Clostridium*-mediated T_{reg} induction is vertically and horizontally transmissible (fig. S10C). *Clostridium* did not affect T_H1 cells but moderately induced T_H17 cells in the colon (fig. S10D). The 46 strains of *Clostridium* have been reported to affect the accumulation of $CD8^+$IELs (intraepithelial lymphocytes) in the colon (*19*). Therefore, *Clostridium* may modulate various aspects of the immune system.

Considering that transforming growth factor–β (TGF-β) is a critical regulator of T_{reg} development, we examined whether *Clostridium* colonization provides a TGF-β–rich environment within the colon. To this end, we cultured whole colons or colonic intestinal epithelial cells (IECs) from GF mice, or mice colonized by either *Clostridium* or *Lactobacillus*, and found a significant increase in the production of active-form TGF-β in the colon and IECs from *Clostridium*-colonized mice (Fig. 2, D and E). Addition of the culture supernatant of IECs from *Clostridium*-colonized mice to splenic $CD4^+$ T cells markedly enhanced the differentiation of Foxp3-expressing cells, and this differentiation was significantly inhibited by an antibody against TGF-β (Fig. 2F). Consistent with the production of TGF-β, transcripts for the genes encoding matrix metalloproteinase 2 (MMP2), MMP9, and MMP13, which have been reported to be involved in the activation of latent TGF-β (*20*), were expressed at higher levels by IECs from *Clostridium*-colonized mice than those from GF or *Lactobacillus*-colonized mice (fig. S11). IECs from *Clostridium*-colonized mice also expressed a high level of indoleamine 2,3-dioxygenase (IDO) (fig. S11), which has been implicated in the induction of T_{regs} (*21*). Collectively, our findings suggest that clostridia activate IECs to produce TGF-β and other T_{reg}-inducing molecules within the colon. We also examined the contribution of bacterial pattern-recognition receptors (PRRs) to the induction of T_{regs} by *Clostridium*. SPF mice deficient for *Myd88* (a signaling adaptor molecule for Toll-like receptors), *Rip2* (an adaptor molecule for NOD receptors), or *Card9* (a key transducer of Dectin-1 signaling) had a normal number of mucosal T_{regs}, compared to each of their littermate controls (fig. S12A). Furthermore, the colonization of GF *Myd88*-deficient mice with *Clostridium* induced

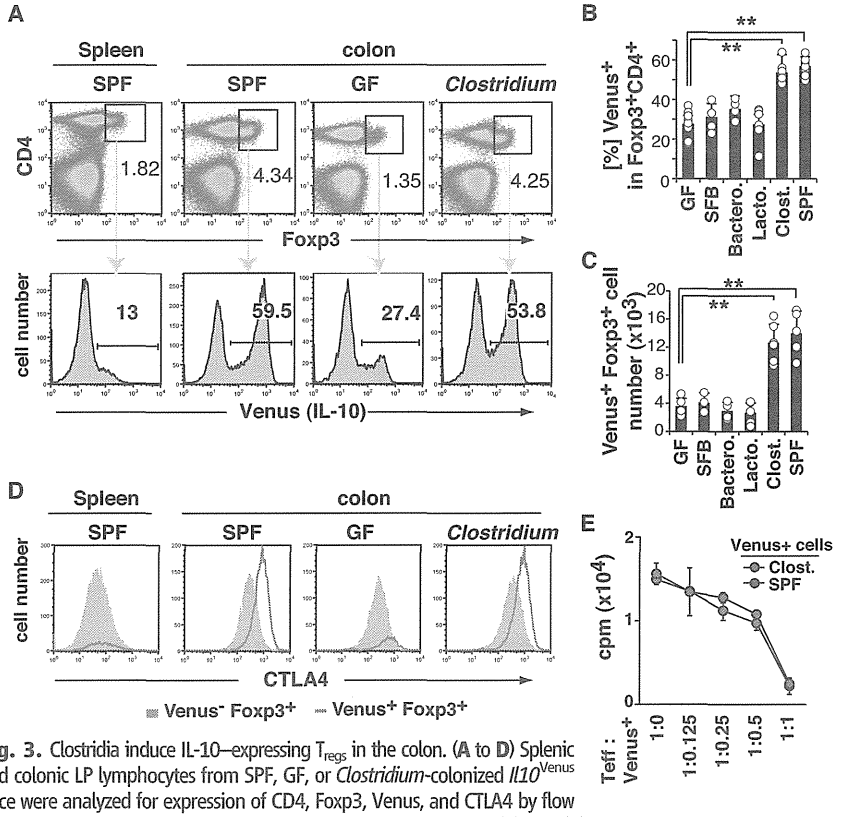

Fig. 3. Clostridia induce IL-10–expressing T_{regs} in the colon. (**A** to **D**) Splenic and colonic LP lymphocytes from SPF, GF, or *Clostridium*-colonized *Il10*^{Venus} mice were analyzed for expression of CD4, Foxp3, Venus, and CTLA4 by flow cytometry. Representative dot-plots and histograms are shown in (A) and (D), and the percentage and absolute number of $Venus^+$ cells within the $CD4^+Foxp3^+$ cell population in individual mice are shown in (B) and (C). Each symbol represents a mouse, and error bars indicate the SD. Data are representative of at least two independent experiments with similar results ($n \geq 5$ mice per group). $^{**}P < 0.001$ versus GF, unpaired *t* test. (**E**) Purified $CD4^+$ $Venus^+$ cells from the colonic LP of SPF or *Clostridium*-colonized *Il10*^{Venus} mice were cultured with splenic $CD4^+CD25^-$ T cells (T_{eff}) in the presence of irradiated splenic $CD11c^+$ cells and anti-CD3 for 72 hours at the indicated ratios. Proliferation was measured by [^{3}H]thymidine uptake. Data represent the mean ± SD of triplicate cultures.

robust accumulation of colonic LP T_{regs} (fig. S12B). These results indicate that clostridia induce T_{regs} independently of these PRR signaling pathways.

Intestinal $Foxp3^+$ T_{regs} exert their immunosuppressive activity, at least in part, through IL-10 production (*22*, *23*). To further probe the nature of T_{regs} induced by *Clostridium*, we newly generated IL-10 reporter mice, in which a cassette containing an internal ribosomal entry site (IRES) and Venus, a brighter version of yellow fluorescent protein, was inserted immediately before the polyadenylation signal of the *Il10* gene (referred to as *Il10*^{Venus} mice; fig. S13). In SPF *Il10*^{Venus} mice, about 60% of $Foxp3^+$ T_{regs} in colonic LP were $Venus^+$, whereas only about 10% of T_{regs} in spleen or other organs were $Venus^+$, consistent with previous studies (*24*, *25*) (Fig. 3, A and B, and fig. S14). Under GF conditions or after antibiotic treatment, the frequency and number of $Venus^+$ cells within the $CD4^+Foxp3^+$ T_{reg} population were significantly lower than those seen under SPF conditions (Fig. 3, A to C, and fig. S15). In contrast, no significant change in the frequency of any regulatory cell components within the $CD4^+$ T cell population in SI LP was observed in the absence, or reduction, of commensal bacteria (fig. S15). These results indicate that the indigenous microflora provide a signal for the accumulation of IL-10^+ T_{regs} in colonic LP, whereas different mechanisms are operating in the induction of $Foxp3^+$- and/or IL-10^+–regulatory cells in SI.

To determine the effect of *Clostridium* on IL-10 expression in colonic T_{regs}, we examined gnotobiotic *Il10*^{Venus} mice colonized with 46 strains of *Clostridium*. The frequency and number of $Venus^+$ cells among $Foxp3^+$ cells in *Il10*^{Venus} mice colonized with *Clostridium* were similar to those in SPF mice (Fig. 3, A to C), indicating that clostridia are sufficient to induce IL-10–expressing $Foxp3^+$ T_{regs}. The induction of IL-10^+ T_{regs} was, again, specifically observed in mice colonized with *Clostridium* but not other bacteria (Fig. 3, B and C). $Venus^+$ $Foxp3^+$ cells in the colonic LP of *Clostridium*-colonized mice expressed high levels of cytotoxic T lymphocyte antigen 4 (CTLA4) (Fig. 3D) and exhibited an in vitro suppressive activity similar to that of $Venus^+$ cells from SPF mice (Fig. 3E). These results indicate that clostridia sufficiently induce the accumulation of functionally competent IL-10^+ $CTLA4^{high}$ T_{regs}. Many of the $Venus^+$ $Foxp3^+$ cells in the colonic LP of SPF and *Clostridium*-colonized mice were found to be negative for Helios, and this cell fraction was particularly reduced in GF mice (fig. S16). These findings suggest that clostridia induce a shift in the composition of T_{regs} in the colonic LP, particularly through accumulation of the IL-10^+ $CTLA4^{high}$ $Helios^-$ subset of T_{regs} (presumably iT_{regs}). Furthermore, 3 weeks after *Clostridium* inoculation, we observed a substantial increase in the number of $Venus^+CD4^+$ cells in the liver, lung, and spleen, where otherwise a very small number of $Venus^+$ cells can be detected (fig. S17). This finding suggests that colonization of *Clostridium* also affects the extra-intestinal immune status.

Early exposure to the environment is known to be a key determinant of adult gut microbial ecology. To affect the *Clostridium* load, we orally inoculated 2-week-old neonatal SPF mice with feces from *Clostridium*-associated mice, kept them under SPF conditions, and examined their microbial composition and T_{reg} number in adulthood. Despite similar amounts of total bacteria in the feces of the *Clostridium*-treated and -untreated groups, there was a significant increase in the amounts of *Clostridium* clusters IV and XIVa in the treated mice (fig. S18A), accompanied by a significantly higher number of colonic $Foxp3^+$ T_{regs} (Fig. 4A). We then examined the effect of abundance of *Clostridium*, and the consequent increase in the number of T_{regs}, on local and systemic immune responses. Mice were subjected to dextran sodium sulfate (DSS)–mediated colitis, a model of colitis resembling human IBD. The symptoms of colitis, such as weight loss and rectal bleeding, were significantly suppressed in *Clostridium*-abundant mice compared with control mice (Fig. 4B). Colon shortening, edema, and hemorrhage were less severe in the colon of *Clostridium*-abundant mice than in that of control mice (Fig. 4C). Consistently, *Clostridium*-abundant mice exhibited milder histological disease characteristics, such as mucosal erosion, cellular infiltration, and crypt loss, than control mice (Fig. 4D). The *Clostridium*-abundant mice were also subjected to oxazolone-induced colitis, an experimental colitis mediated by T_H2-type cells (*26*). *Clostridium*-abundant mice had attenuated weight loss and fewer areas of mucosal erosion, edema, cellular infiltration, and hemorrhage (fig. S18, B and C). Finally, we investigated the effect of *Clostridium* on systemic immunoglobulin E (IgE) production. Ovalbumin (OVA)–specific IgE levels in sera were measured after intraperitoneal injection of alum-absorbed OVA. *Clostridium*-abundant mice showed significantly lower IgE levels than control mice (Fig. 4E). Moreover, splenocytes from *Clostridium*-abundant mice immunized with OVA plus alum showed lower IL-4 and higher IL-10 productions after restimulation with OVA

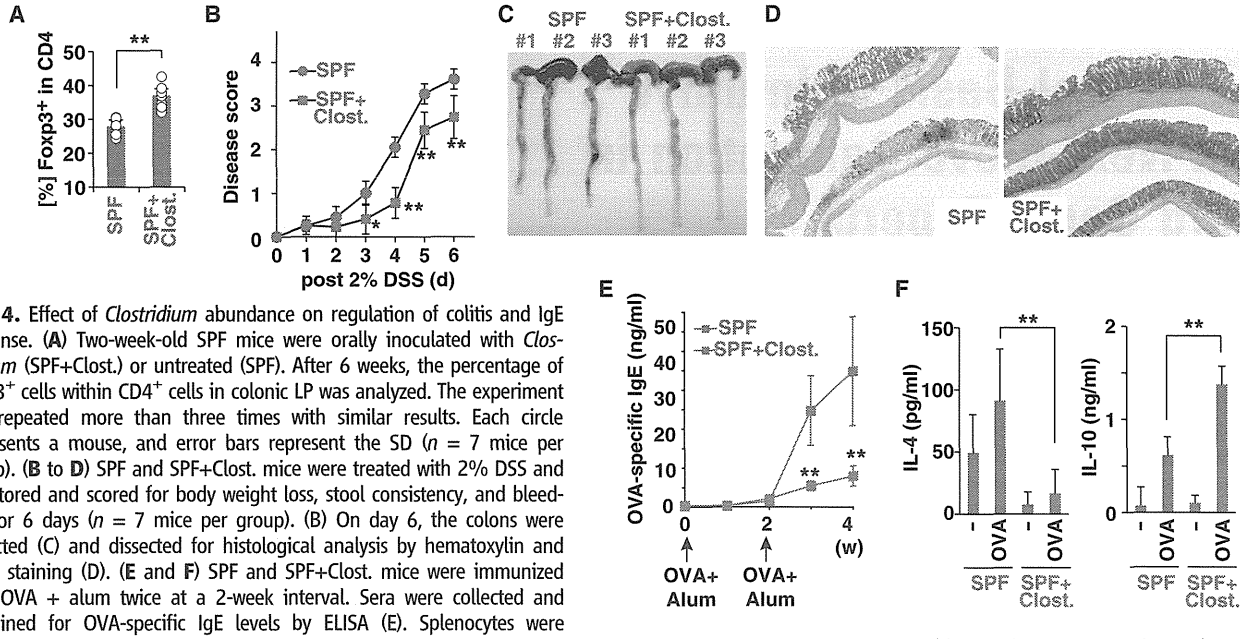

Fig. 4. Effect of *Clostridium* abundance on regulation of colitis and IgE response. (**A**) Two-week-old SPF mice were orally inoculated with *Clostridium* (SPF+Clost.) or untreated (SPF). After 6 weeks, the percentage of $Foxp3^+$ cells within $CD4^+$ cells in colonic LP was analyzed. The experiment was repeated more than three times with similar results. Each circle represents a mouse, and error bars represent the SD (n = 7 mice per group). (**B** to **D**) SPF and SPF+Clost. mice were treated with 2% DSS and monitored and scored for body weight loss, stool consistency, and bleeding for 6 days (n = 7 mice per group). (B) On day 6, the colons were collected (C) and dissected for histological analysis by hematoxylin and eosin staining (D). (**E** and **F**) SPF and SPF+Clost. mice were immunized with OVA + alum twice at a 2-week interval. Sera were collected and examined for OVA-specific IgE levels by ELISA (E). Splenocytes were collected from mice in each group and examined for IL-4 and IL-10 production upon restimulation with OVA in vitro (F). Error bars represent the SD (n = 5 mice per group). *P < 0.02; **P < 0.001, unpaired t test.

in vitro than those from control mice (Fig. 4F). Therefore, the increased the proportion of *Clostridium* in the gut microbiota affected mucosal inflammation and systemic antibody responses. Although additional mechanisms and cell types could be involved, our findings suggest that *Clostridium*-mediated induction of T_{regs} in the colon may be responsible for these effects.

Our findings show that T_{regs} are abundant in intestinal LP, and their accumulation in the SI and colon is differentially regulated. The induction of colonic T_{regs} is dependent on commensal microorganisms with specialized properties. Among the indigenous commensal bacteria, *Clostridium* spp. belonging to clusters IV and XIVa are outstanding inducers of T_{regs} in the colon. Although alternative mechanisms may also be involved, our findings are consistent with a model in which the presence of *Clostridium* induces the release of active TGF-β and other T_{reg}-inducing factors from IECs, which presumably cooperate with dendritic cells to induce a general accumulation of T_{regs} in the colon and at the same time affect the proportions of individual T_{reg} subsets through the preferential induction of IL-10^+ CTLA4^{high} iT_{regs}. Several recent studies have focused on the microbial composition in the intestine during health and disease. Notably, *Clostridium* clusters IV and XIVa constitute a smaller proportion of the fecal community in patients with IBD than in healthy controls (*15*). Furthermore, some patients with IBD have a specific reduction in *Faecalibacterium prausnitzii*, a bacterium belonging to *Clostridium* cluster IV (*16*). These reports are consistent with our findings and raise the possibility that indigenous *Clostridium*-dependent induction of T_{regs} may be required for maintaining immune homeostasis in mice and humans. The factors derived from *Clostridium* that are required for the induction of mucosal T_{regs} are currently unknown. Because gnotobiotic mice colonized with three strains of *Clostridium* showed an intermediate pattern of T_{reg} induction between GF mice and mice inoculated with all 46 strains (fig. S19), we speculate that a diverse set of metabolites that are most efficiently produced by the 46 strains of *Clostridium* as a whole may be required for the optimal induction of T_{regs}. Identifying these metabolites and the molecular mechanisms underlying the *Clostridium*-host crosstalk will provide invaluable information toward understanding how the gut microbiota regulates immune homeostasis and may suggest potential therapeutic options for treating human IBD and allergies.

References and Notes

1. A. J. Macpherson, N. L. Harris, *Nat. Rev. Immunol.* **4**, 478 (2004).
2. J. L. Round, S. K. Mazmanian, *Nat. Rev. Immunol.* **9**, 313 (2009).
3. I. I. Ivanov *et al.*, *Cell* **139**, 485 (2009).
4. V. Gaboriau-Routhiau *et al.*, *Immunity* **31**, 677 (2009).
5. H. J. Wu *et al.*, *Immunity* **32**, 815 (2010).
6. J. A. Hall *et al.*, *Immunity* **29**, 637 (2008).
7. C. Di Giacinto, M. Marinaro, M. Sanchez, W. Strober, M. Boirivant, *J. Immunol.* **174**, 3237 (2005).
8. K. Karimi, M. D. Inman, J. Bienenstock, P. Forsythe, *Am. J. Respir. Crit. Care Med.* **179**, 186 (2009).
9. A. Lyons *et al.*, *Clin. Exp. Allergy* **40**, 811 (2010).
10. J. L. Round, S. K. Mazmanian, *Proc. Natl. Acad. Sci. U.S.A.* **107**, 12204 (2010).
11. W. S. Garrett, J. I. Gordon, L. H. Glimcher, *Cell* **140**, 859 (2010).
12. I. I. Ivanov *et al.*, *Cell Host Microbe* **4**, 337 (2008).
13. B. Min *et al.*, *Eur. J. Immunol.* **37**, 1916 (2007).
14. Y. Momose, A. Maruyama, T. Iwasaki, Y. Miyamoto, K. Itoh, *J. Appl. Microbiol.* **107**, 2088 (2009).
15. D. N. Frank *et al.*, *Proc. Natl. Acad. Sci. U.S.A.* **104**, 13780 (2007).
16. H. Sokol *et al.*, *Inflamm. Bowel Dis.* **15**, 1183 (2009).
17. K. Itoh, T. Mitsuoka, *Lab. Anim.* **19**, 111 (1985).
18. A. M. Thornton *et al.*, *J. Immunol.* **184**, 3433 (2010).
19. Y. Umesaki, H. Setoyama, S. Matsumoto, A. Imaoka, K. Itoh, *Infect. Immun.* **67**, 3504 (1999).
20. M. D'Angelo, P. C. Billings, M. Pacifici, P. S. Leboy, T. Kirsch, *J. Biol. Chem.* **276**, 11347 (2001).
21. G. Matteoli *et al.*, *Gut* **59**, 595 (2010).
22. M. J. Barnes, F. Powrie, *Immunity* **31**, 401 (2009).
23. Y. P. Rubtsov *et al.*, *Immunity* **28**, 546 (2008).
24. M. Kamanaka *et al.*, *Immunity* **25**, 941 (2006).
25. C. L. Maynard *et al.*, *Nat. Immunol.* **8**, 931 (2007).
26. M. Boirivant, I. J. Fuss, A. Chu, W. Strober, *J. Exp. Med.* **188**, 1929 (1998).

27. We thank Y. Ueda, J. Nishimura, and H. Saiga for technical assistance, R. Eisenman for critically reading the manuscript, and A. Miyawaki for Venus. We thank the staff at the Sankyo Laboratories for gnotobiotic handling of the mice. The work was supported by Grants-in-Aid for Scientific Research from the Ministry of Education, Culture, Sports, Science and Technology, Core Research for Evolutional Science and Technology (CREST), Japan Science and Technology, the Mochida Memorial Foundation for Medical and Pharmaceutical Research, the Kato Memorial Bioscience Foundation, the Mishima Kaiun Memorial Foundation, Kanae Foundation for the Promotion of Medical Science, and Inoue Foundation for Science. The authors have applied for a patent for use of bacteria belonging to the genus *Clostridium* or a physiologically active substance derived from these bacteria to induce proliferation or accumulation of regulatory T cells and suppress immune functions (patent application no. JP 2010-129134). *Material transfer agreements are required for the use* of the IL-10 Venus mice, SFB, *Clostridium* spp. 46 strains, *Bacteroides* spp. 16 strains, and *Lactobacillus* spp. 3 strains.

Supporting Online Material

www.sciencemag.org/cgi/content/full/science.1198469/DC1
Materials and Methods
Figs. S1 to S19
References

29 September 2010; accepted 1 December 2010
Published online 23 December 2010;
10.1126/science.1198469

The Neural Basis of Intuitive Best Next-Move Generation in Board Game Experts

Xiaohong Wan,[1] Hironori Nakatani,[1] Kenichi Ueno,[2] Takeshi Asamizuya,[2] Kang Cheng,[1,2] Keiji Tanaka[1]*

The superior capability of cognitive experts largely depends on quick automatic processes. To reveal their neural bases, we used functional magnetic resonance imaging to study brain activity of professional and amateur players in a board game named shogi. We found two activations specific to professionals: one in the precuneus of the parietal lobe during perception of board patterns, and the other in the caudate nucleus of the basal ganglia during quick generation of the best next move. Activities at these two sites covaried in relevant tasks. These results suggest that the precuneus-caudate circuit implements the automatic, yet complicated, processes of board-pattern perception and next-move generation in board game experts.

Board games provide a good opportunity to study the mechanisms underlying cognitive expertise because these games are played in accordance with a set of well-defined rules. There is a history of psychological studies of chess over the last 100 years (*1*–*3*). In an early study (*4*), both world-class and local-club players were asked to think aloud while playing, and no difference was found in the depth or width of search between the two groups. Instead, a difference was found in the selection of game tree branches that the player put into the search process: The best next move was always included in the first part of search in world-class players, whereas local-club players often missed it in their large search. de Groot inferred that world-class players generate one or a few best next moves mainly by cued recall (*4*). Subsequently, on the basis of the experts' superior performance in the board-pattern recall task it was proposed that chess experts quickly perceive chess patterns using various stereotyped arrangements of several

[1]Cognitive Brain Mapping Laboratory, RIKEN Brain Science Institute, 2-1 Hirosawa, Wako, Saitama 351-0198, Japan. [2]Support Unit for Functional Magnetic Resonance Imaging, RIKEN Brain Science Institute, 2-1 Hirosawa, Wako, Saitama 351-0198, Japan.

*To whom correspondence should be addressed. E-mail: keiji@riken.jp

TECHNICAL REPORTS

nature medicine

Functional engraftment of colon epithelium expanded *in vitro* from a single adult Lgr5$^+$ stem cell

Shiro Yui[1,6], Tetsuya Nakamura[2,6], Toshiro Sato[3,5], Yasuhiro Nemoto[1], Tomohiro Mizutani[1], Xiu Zheng[1], Shizuko Ichinose[4], Takashi Nagaishi[1], Ryuichi Okamoto[2], Kiichiro Tsuchiya[1], Hans Clevers[3] & Mamoru Watanabe[1]

Adult stem-cell therapy holds promise for the treatment of gastrointestinal diseases. Here we describe methods for long-term expansion of colonic stem cells positive for leucine-rich repeat containing G protein-coupled receptor 5 (Lgr5$^+$ cells) in culture. To test the transplantability of these cells, we reintroduced cultured GFP$^+$ colon organoids into superficially damaged mouse colon. The transplanted donor cells readily integrated into the mouse colon, covering the area that lacked epithelium as a result of the introduced damage in recipient mice. At 4 weeks after transplantation, the donor-derived cells constituted a single-layered epithelium, which formed self-renewing crypts that were functionally and histologically normal. Moreover, we observed long-term (>6 months) engraftment with transplantation of organoids derived from a single Lgr5$^+$ colon stem cell after extensive *in vitro* expansion. These data show the feasibility of colon stem-cell therapy based on the *in vitro* expansion of a single adult colonic stem cell.

Epithelial stem cells maintain tissue homeostasis throughout the gastrointestinal tract[1–3]. The Wnt, bone morphogenetic protein (BMP) and Notch cascades function together to regulate stem-cell maintenance[4,5]. *Lgr5* marks stem cells in small intestinal and colonic crypts[6] and in gastric units[7]. *Bmi1* may mark distinct stem cells in the proximal small intestine[8]. It has been shown that freshly isolated intestinal epithelium can be transplanted in rodents after resident epithelium has been surgically removed[9,10]. We previously developed a three-dimensional culture technique that allows expansion of single Lgr5$^+$ stem cells from small intestine[11], stomach[7] and colon[12]. The resulting organoids then expand and self organize into an epithelial architecture that is reminiscent of that seen in *in vivo* histology. Moreover, the growing organoids maintain their tissue identity even after prolonged culture. Here we sought to evaluate whether the cultured Lgr5$^+$ cells faithfully represent the tissue-resident Lgr5$^+$ stem cells and, thus, are able to regenerate epithelial tissue *in vivo*. Considering that the colon is very vulnerable to disease in humans, we focused on colonic stem cells in our analyses.

RESULTS

Long-term, serum-free culture system for colonic organoids

We subjected the colons of adult mice to a combination of enzymes[13], reducing agents[14] and mechanical disruption. The resulting crypt fragments were mostly devoid of α smooth muscle actin gene (*Acta2*)-expression–positive non-epithelial components and consisted of a mix of cadherin 1, type 1, E-cadherin (*Cdh1*)$^+$ cells expressing terminal differentiation marker genes (*Muc2*, *CA2* and *ChgA*) and Lgr5$^+$ stem cells (**Supplementary Fig. 1a,b**).

The addition of R-spondin 1 (Rspo1), Noggin and epidermal growth factor (EGF), which are all essential to small intestine culture[11], did not maintain the growth of colonic crypts. We therefore developed the following 'TMDU (Tokyo Medical and Dental University) protocol': we embedded crypts in type I collagen in serum-free medium with Wnt3a, hepatocyte growth factor (HGF)[15,16] and BSA, in addition to Rspo1, Noggin and EGF (**Supplementary Fig. 1c**). Sequential imaging of the cultures revealed rapid growth of cystic structures (**Fig. 1a**). Wnt3a, Rspo1 and BSA were essential to this growth (**Supplementary Fig. 1d**). As predicted by previous results[17,18], Rspo1 could be substituted with Wnt3a (data not shown). Although Noggin, EGF and HGF were not essential for growth of the colonic crypts, each enhanced their growth (**Supplementary Fig. 1e**). The colonic organoids rarely had buds (**Fig. 1a**, **Supplementary Fig. 2a** and **Supplementary Video 1**). Of note, small intestinal organoids also generate cystic structures when Wnt3a is added to them[19].

The colonic organoids were single layered (**Supplementary Fig. 2b**), and all the cells within were positive for Cdh1 expression (**Fig. 1b**). The basal membranes of the organoids faced outward (**Fig. 1b**). Ki67$^+$ cells were present in the colonic organoids (**Fig. 1b**), as were alcian blue–positive goblet cells, chromogranin A (ChgA)$^+$ enteroendocrine cells, carbonic anhydrase II (CA2)$^+$ colonocytes and cytochrome c oxidase subunit I (COX1)$^+$ tuft cells[20] (**Fig. 1b**). Transmission electron microscopy revealed epithelial characteristics such as microvilli (**Fig. 1c**) and junctional complexes (**Fig. 1d**) in the organoids. However, stromal cells were absent (**Supplementary Fig. 2c**). Mitotic cells with condensed chromosomes were present in the organoids (**Fig. 1e**), and goblet cells (**Fig. 1f**) and enteroendocrine cells (**Fig. 1g**) could also be clearly detected.

[1]Department of Gastroenterology and Hepatology, Graduate School, Tokyo Medical and Dental University, Bunkyo-ku, Tokyo, Japan. [2]Department of Advanced Therapeutics for Gastrointestinal Diseases, Tokyo Medical and Dental University, Bunkyo-ku, Tokyo, Japan. [3]Hubrecht Institute and University Medical Centre, Utrecht, The Netherlands. [4]Research Center for Medical and Dental Sciences, Tokyo Medical and Dental University, Bunkyo-ku, Tokyo, Japan. [5]Present address: Department of Gastroenterology, Keio University School of Medicine, Shinjuku-ku, Tokyo, Japan. [6]These authors contributed equally to this work. Correspondence should be addressed to H.C. (h.clevers@hubrecht.eu) or M.W. (mamoru.gast@tmd.ac.jp).

Received 30 July 2011; accepted 29 November 2011; published online 11 March 2012; doi:10.1038/nm.2695

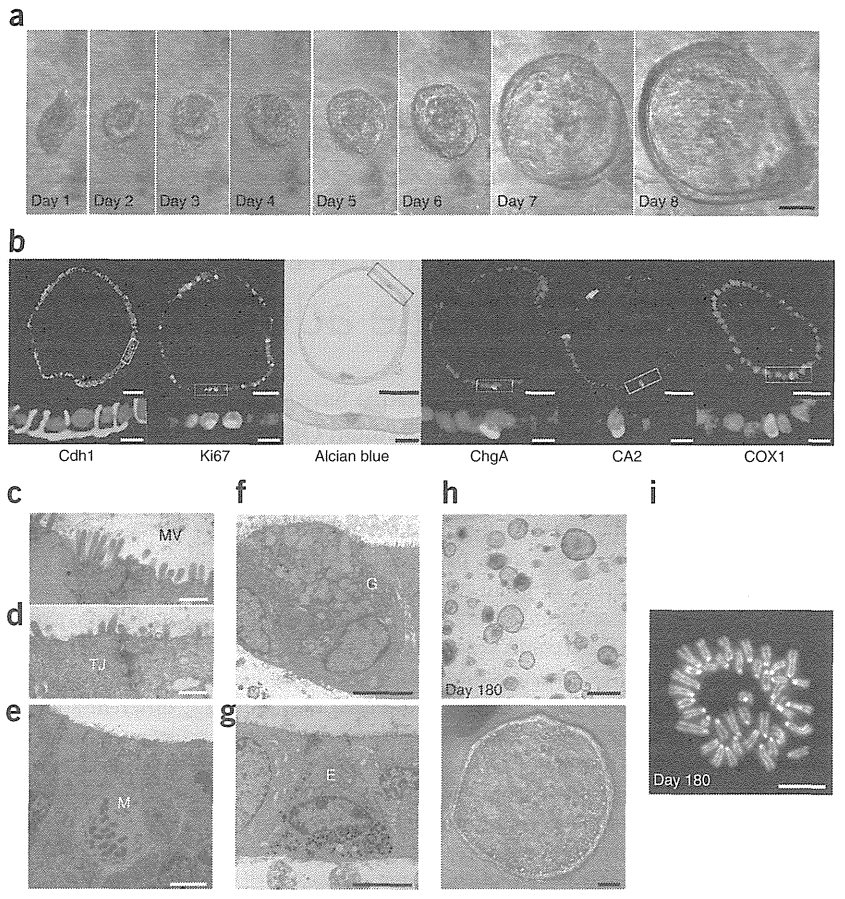

Figure 1 Long-term, serum-free culture of colonic epithelial cells. (**a**) A representative colonic crypt growing as a cystic structure. Scale bar, 50 μm. Time-lapse images of another colonic crypt are shown in **Supplementary Figure 2a** and **Supplementary Video 1**. (**b**) Histology of the colonic organoids at day 8 of culture. Cdh1$^+$ cells, actively proliferating Ki67$^+$ cells (green) and terminally differentiated cells stained with alcian blue (blue, goblet cells) or immunostained with ChgA (green, enteroendocrine cells), CA2 (green, colonocytes) or COX1 (green, tuft cells) are shown. Higher magnification views of the boxed areas are shown at the bottom. DAPI staining was performed, except for the experiments in which we performed alcian blue staining. Scale bars, top, 50 μm; bottom, 10 μm. (**c**–**g**) Transmission electron microscopy analysis for organoids at day 8. (**c**,**d**) Microvilli (MV) and intracellular tight junctions (TJ) are shown. (**e**) Mitotic (M) cells showing chromatin condensation. (**f**,**g**) Goblet cells (G) with mucus granules (**f**) and enteroendocrine cells (E) with electron dense granules (**g**) are shown. Scale bars: **c**,**d**, 0.5 μm; **e**–**g**, 5 μm. Low-power views of **f** and **g** are also shown in **Supplementary Figure 2c**. (**h**) The culture at day 180 (top) and its representative organoid (bottom). Scale bars, top, 500 μm; bottom, 50 μm. Images of the growth of a single cell after passage are shown in **Supplementary Figure 3** and **Supplementary Video 2**. (**i**) Metaphase spread of a cell at day 180 shows a normal karyotype ($2n = 40$). Scale bar, 10 μm.

The organoids could be passaged weekly at a 1:2 ratio (**Supplementary Fig. 3** and **Supplementary Video 2**). Addition of the Rho kinase inhibitor Y-27632 (ref. 21) improved the replating efficiency of the organoids[11]. We successfully propagated organoids for more than 6 months without clear alterations of morphology (**Fig. 1h**) or karyotype (**Fig. 1i**).

Lgr5$^+$ cells are enriched in colonic organoids

We tracked the expression of *Lgr5* over 60 d and found a substantial elevation during the first 8 d of observation (**Fig. 2a**). We found no change in the expression of *ChgA* and *CA2*, whereas *Muc2* expression was repressed in the first 8 d (**Fig. 2a**). Addition of a combination of Wnt3a, Rspo1 and BSA induced *Lgr5* expression (**Fig. 2b**). *Lgr5* expression was further upregulated by the addition of Noggin, which is an antagonist of BMP[22] (**Fig. 2b**). The Notch pathway suppresses the

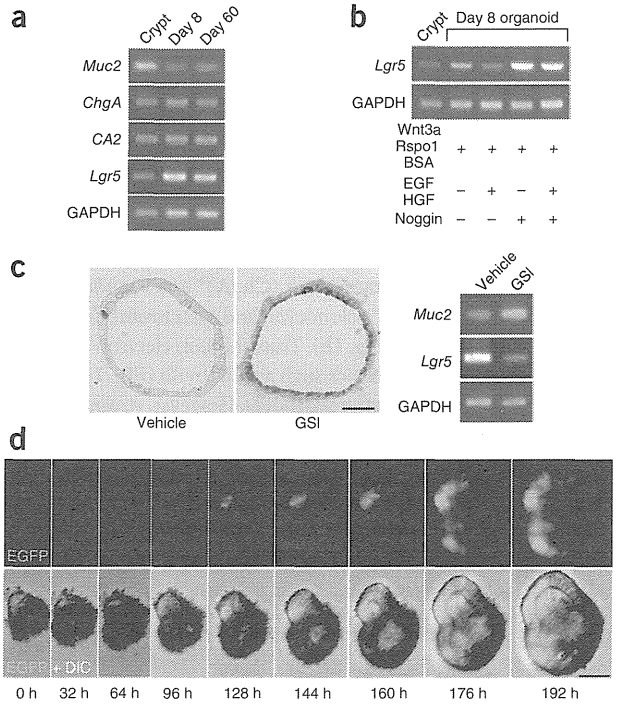

Figure 2 Lgr5$^+$ stem cells are enriched in cultured organoids. (**a**) RT-PCR analysis of the colonic crypts immediately after isolation (crypt) or organoids cultured for 8 or 60 d. *Lgr5* was upregulated and stayed constant thereafter. Differentiation marker genes (*Muc2*, *ChgA* and *CA2*) were expressed over 60 d. The primers used are listed in **Supplementary Table 1**. (**b**) RT-PCR shows that *Lgr5* upregulation is mediated by a combination of minimum factors (Wnt3a, Rspo1 and BSA) and Noggin but not by EGF and HGF. (**c**) Notch signal-mediated cell fate determination *in vitro*. Cultured organoids were treated with GSI, LY-411575 or vehicle alone from day 4 to day 8. Organoids stained with alcian blue are shown (left). Scale bar, 50 μm. RT-PCR shows that the expression of *Muc2* is upregulated, whereas the expression of *Lgr5* is reciprocally downregulated in organoids treated with LY-411575 (GSI, right). Similar results were obtained in three independent experiments, and representative data are shown. (**d**) A time-lapse imaging of a growing colonic crypt obtained from an *Lgr5-EGFP-ires-CreERT2* mouse over 192 h. The top panel shows EGFP and the bottom panel shows merged images of EGFP and differential interference contrast (DIC). Scale bar, 50 μm. The corresponding video (**Supplementary Video 3**) and similar results from another example are available as **Supplementary Figure 4a** and **Supplementary Video 4**.

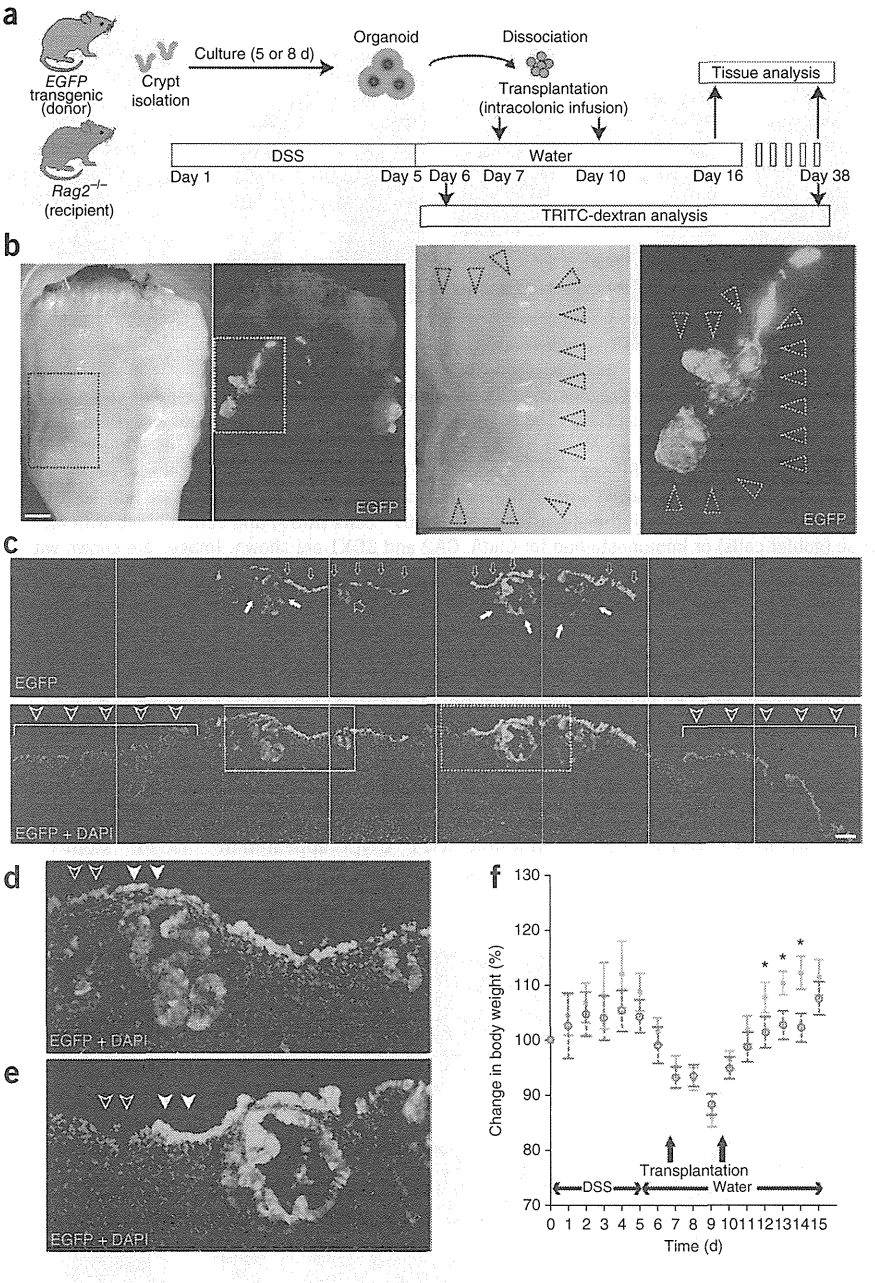

Figure 3 Transplantation of cultured cells improves acute colitis. (**a**) Experimental protocols. (**b**) Recipient colon at 6 d after transplantation. Low-power views (stereoscopic and fluorescent images) are shown on the left. High-power views of the areas in the dotted squares are shown in the right. The black dotted arrowheads show a depressed area surrounded by edematous mucosa. EGFP$^+$ areas overlapping the damaged region (white dotted arrowheads) are also shown. Note that the outline of the tissue is not precisely the same in the stereoscopic and fluorescent images, as they were acquired on different microscopes. Scale bars, 1 mm. (**c**) Histology of the EGFP$^+$ area shown in **b**. EGFP (top) and the merged image with DAPI staining (bottom). EGFP$^+$ cells cover the damaged mucosa that intervene separate areas preserving crypt structures (bottom, arrowheads). EGFP$^+$ cells constitute flat linings (top, narrow open arrow) or an invagination (top, wide open arrows), the latter of which is reminiscent of crypts. EGFP$^+$ cystic structures were also observed in the EGFP$^+$ cells (top, filled white arrows). The regions in the solid- and dotted-line boxes are shown at higher magnification in **d** and **e**, respectively. Scale bar, 100 μm. (**d**) High-power view of the solid box in **c**. (**e**) High-power view of the dotted box in **c**. (**f**) *Rag2*$^{-/-}$ mice were given DSS for 5 d, and then transplantation ($n = 6$) or sham-transplantion ($n = 6$) was performed. On day 16, the presence of engraftment was retrospectively assessed after the mice were killed. The body weights of the mice with EGFP$^+$ engraftment (green squares, $n = 4$) and sham-transplanted controls (red open circles, $n = 6$) are presented as a percentage of their initial weight. Error bars, s.e.m. $^*P < 0.05$ (Student's *t* test).

differentiation of progenitors[23,24] and stem cells[25] toward secretory lineages. We treated the colonic organoids with LY-411575, a γ-secretase inhibitor (GSI) that is capable of inhibiting Notch signaling[26,27]. Notch inhibition induced a goblet-cell phenotype with an increased level of *Muc2* mRNA and a reciprocal decrease in the expression of *Lgr5* (**Fig. 2c**).

We next performed live imaging of colonic organoids obtained from *Lgr5-EGFP-internal ribosome entry site (ires)-CreERT2* mice[6] in which an enhanced GFP (EGFP) and tamoxifen-inducible Cre recombinase cassette is integrated into the *Lgr5* locus. The *Lgr5*-promoter–driven EGFP expression initially stayed at a marginal level but then increased beginning at day 5 (**Fig. 2d**, **Supplementary Fig. 4a** and **Supplementary Videos 3** and **4**). We confirmed the expansion of Lgr5$^+$ cells at a single-cell resolution (**Supplementary Fig. 4b**). Over multiple passages, the *Lgr5-EGFP* locus tended to become silenced, whereas the wild-type *Lgr5* allele remained active (**Fig. 2a,b**). Taken together, colonic Lgr5$^+$ stem cells were able to self renew and expand *in vitro*.

Cultured colonic organoids rescue damaged epithelium

We next tested the transplantability of the cultured organoids (**Fig. 3a**). We induced colonic mucosal damage by providing immunocompromised *Rag2*$^{-/-}$ mice with colitis-inducing dextran sulfate sodium (DSS)[28] for 5 d. Most of the mice developed acute colitis characterized by weight loss, bloody stool, diarrhea and epithelial injury in the distal colon. At 7 and 10 d after initiating DSS administration, we dissociated the organoids cultured from *EGFP* transgenic mice[29] into small fragments, suspended them in a Matrigel-containing PBS and instilled them by enema in recipient mice.

At 16 d after the start of DSS administration, the recipient colons showed varying degrees of recovery. Multiple EGFP$^+$ areas appeared as well-demarcated patches in the treated colons (**Fig. 3b**). We did not observe any EGFP$^+$ areas in colons not treated with DSS (data not shown). Histologically, the EGFP$^+$ cells covered the submucosa and were located between the less damaged recipient tissues (**Fig. 3c**). The EGFP$^+$ cells formed flat or slightly invaginated linings (**Fig. 3c**). We also observed large cystic EGFP$^+$ structures below the surface of the treated colons (**Fig. 3c**). Some of the EGFP$^+$ areas connected to the recipients' epithelium (**Fig. 3d**), whereas others repopulated areas that were devoid of recipient epithelium (**Fig. 3e**). Notably, the body weights of the mice with engraftment were

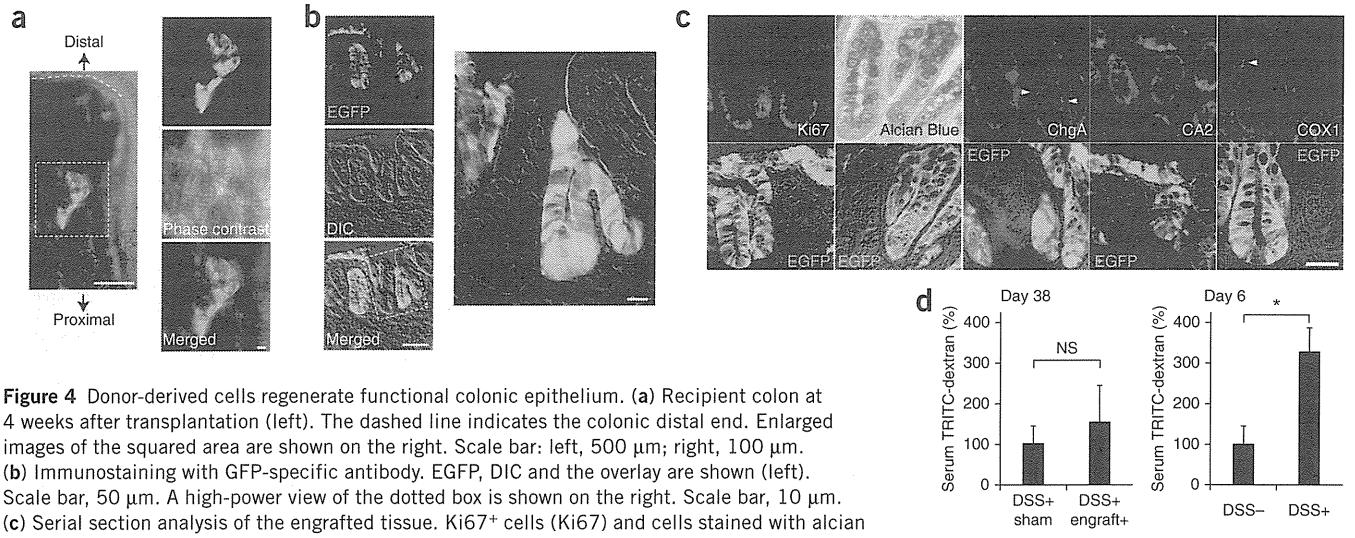

Figure 4 Donor-derived cells regenerate functional colonic epithelium. (**a**) Recipient colon at 4 weeks after transplantation (left). The dashed line indicates the colonic distal end. Enlarged images of the squared area are shown on the right. Scale bar: left, 500 μm; right, 100 μm. (**b**) Immunostaining with GFP-specific antibody. EGFP, DIC and the overlay are shown (left). Scale bar, 50 μm. A high-power view of the dotted box is shown on the right. Scale bar, 10 μm. (**c**) Serial section analysis of the engrafted tissue. Ki67$^+$ cells (Ki67) and cells stained with alcian blue (goblet cells) or immunostained for ChgA, CA2 and COX1 are shown. Images are shown with or without DAPI staining. The bottom row shows neighboring sections stained for GFP. Arrowheads point to ChgA$^+$ or COX1$^+$ cells. Scale bar, 50 μm. (**d**) After DSS colitis induction, transplantation ($n = 6$) or sham transplantation ($n = 6$) was performed. Mice were administered TRITC-dextran by gavage before killing on day 38. Four out of six colons in the transplanted group had EGFP$^+$ engraftment, and the serum TRITC concentration in these mice is shown (DSS+ engraft+; $n = 4$) as a percentage of that in the sham-transplanted group (DSS+ sham; $n = 6$). As a control, DSS colitis was induced (DSS+; $n = 6$) or uninduced (DSS–; $n = 6$) in *Rag2*$^{-/-}$ mice, and these mice were subjected for the same assay on day 6 without transplantation. Data are shown as a percentage of the concentrations in uninduced mice. Error bars, s.e.m. $^*P < 0.05$, NS, not significant (Student's *t* test).

higher than those of sham-transplanted mice (**Fig. 3f**; with statistically significant results at days 12, 13 and 14, $P < 0.05$).

At 4 weeks after transplantation, tube-like EGFP$^+$ crypts appeared in the distal colon (**Fig. 4a**) that were morphologically indistinguishable from the surrounding EGFP$^-$ epithelium (**Fig. 4b**). Notably, the engrafted crypts were entirely EGFP$^+$, indicating the presence of EGFP$^+$ stem cells (**Fig. 4b**). Cells in the lower part of the EGFP$^+$ crypts were normally Ki67$^+$, and the EGFP$^+$ crypts contained all

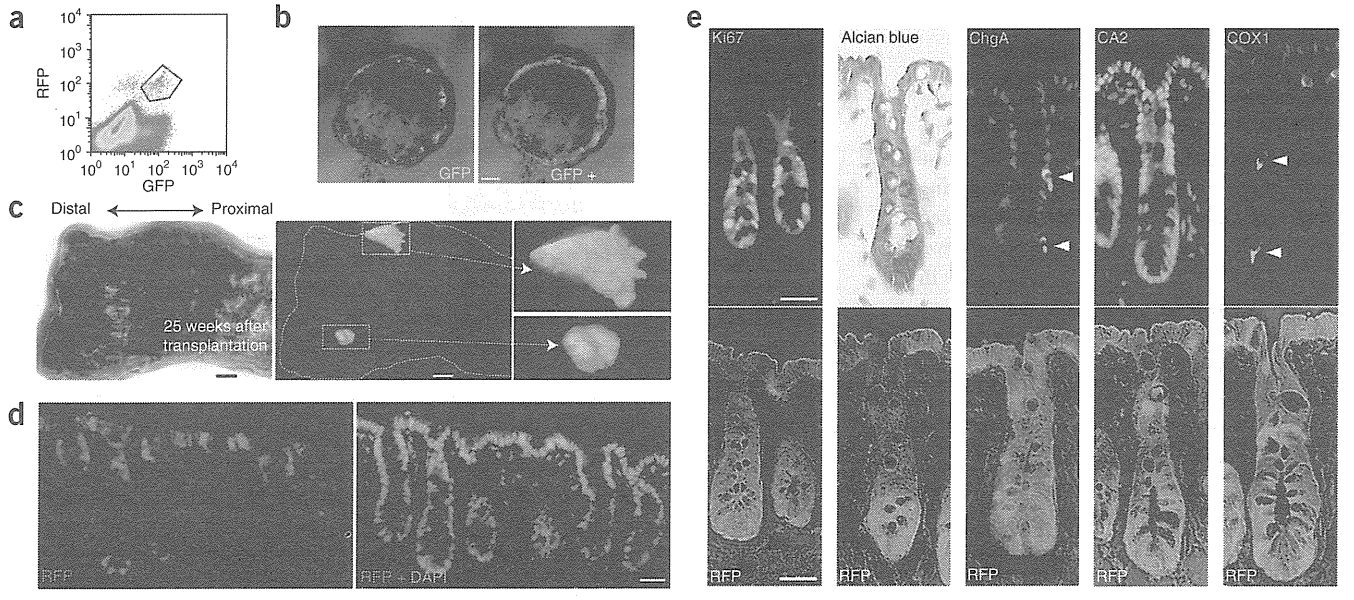

Figure 5 Single Lgr5$^+$ stem-cell–derived cultured cells serve as long-lived, multipotential stem cells *in vivo*. (**a**) Fluorescence-activated cell sorting analysis of colonic cells of *R26R-Confetti* mice crossed with *Lgr5-EGFP-ires-CreERT2* mice 3 d after Cre induction. The EGFP$^+$ and RFP$^+$ populations located in the box were sorted and cultured. (**b**) Images are shown of one out of four organoids grown from sorted single Lgr5$^+$ cells at day 6. EGFP$^+$ stem cells are scattered in the organoid (left), with all the offspring being positive for RFP (right). Scale bar, 50 μm. (**c**) Images of the recipient colon at 25 weeks after transplantation. The phase-contrast view of the recipient colon is shown on the left. The fluorescent image shows the tissue contains RFP$^+$ grafts (right). Scale bar, 1 mm. Enlarged images of the boxed areas are also shown (2.7-fold magnification). (**d**) Immunostaining of the RFP$^+$ engraft at 25 weeks after transplantation. An image of RFP-specific antibody staining (left) and an image of RFP staining merged with DAPI staining (right) are shown. Scale bar, 50 μm. (**e**) Serial section analysis of the engrafted RFP$^+$ tissue at 25 weeks after transplantation. The top panels show Ki67, alcian blue, ChgA, CA2 or COX1 staining with or without nuclei stained by DAPI. The bottom panels show the adjacent sections stained for RFP. Arrowheads point to ChgA$^+$ enteroendocrine cells and COX1$^+$ tuft cells. Scale bars, 50 μm.